

Far-infrared magneto-optical study of two-dimensional electrons and holes in InAs/Al_xGa_{1-x}Sb quantum wells

J. Kono* and B. D. McCombe†

Department of Physics, State University of New York at Buffalo, Buffalo, New York 14260

J.-P. Cheng‡

Francis Bitter National Magnet Laboratory, Massachusetts Institute of Technology, Cambridge, Massachusetts 02139

I. Lo,§ W. C. Mitchel, and C. E. Stutz

Wright Laboratory, Wright-Patterson Air Force Base, Dayton, Ohio 45433-6533

(Received 6 May 1996; revised manuscript received 15 July 1996)

We present results of a detailed far-infrared magneto-optical study on a series of high-mobility InAs/Al_xGa_{1-x}Sb ($x=1.0, 0.8, 0.5, 0.4, 0.2,$ and 0.1) type-II single quantum wells. A wide range of phenomena arising from the unusual properties of two-dimensional (2D) electrons and holes and their Coulomb interaction in high magnetic fields has been revealed. Semiconducting samples ($x \geq 0.4$), in which only 2D electrons exist in the InAs wells, exhibit cyclotron-resonance (CR) splittings due to large conduction-band nonparabolicity. Semimetallic samples ($x=0.1$ and 0.2), in which both 2D electrons (in InAs) and 2D holes (in Al_xGa_{1-x}Sb) are present, show two additional lines (e and h - X lines) as well as electron and hole CR. The X -lines increase in intensity at the expense of CR with increasing electron-hole (e - h) pair density, decreasing temperature, or increasing magnetic field (at low field), suggesting that they are associated with e - h binding which is increased by the magnetic field. The electron CR shows strongly oscillatory linewidth, amplitude, and mass, part of which are interpreted in the light of the unusual ‘‘antinonparabolic’’ band structure resulting from band overlap and coupling between conduction-band states in InAs and valence-band states in Al_xGa_{1-x}Sb; part of these results are qualitatively consistent with the predictions of Altarelli and co-workers. The X lines are attributed to internal transitions of correlated electron e - h pairs (excitons) in high magnetic fields mediated by the excess electron density. [S0163-1829(97)04403-2]

I. INTRODUCTION

Semiconductor heterostructures made from the combination of InAs and Al_xGa_{1-x}Sb have been of considerable interest for the past two decades because of their unusual band-edge alignment,¹ due to which electrons and holes are spatially separated and confined in different layers. Interest in this material system has also been stimulated by the large nonparabolicity, small mass, and large g factor of the electrons contained in the InAs layers, compared to commonly used GaAs/Al_xGa_{1-x}As systems, as well as possible applications as infrared detectors and sources. Until recently, however, systematic experimental studies of intrinsic properties of this system had been limited to the end member InAs/GaSb,² primarily due to the difficulty in growing high-mobility, impurity-free samples. The past several years have seen remarkable progress in the growth of InAs/Al_xGa_{1-x}Sb quantum-well (QW) structures with high-mobility ($>10^5$ cm²/V s) two-dimensional (2D) carriers.³⁻⁵ This has led to such experimental observations as zero-field spin splitting due to asymmetric potential wells,⁶ magnetic-field-induced semimetal-semiconductor transitions,⁷⁻⁹ cyclotron-resonance (CR) splittings due to nonparabolicity,^{10,11} strong CR oscillations,¹² far-infrared (FIR) transitions attributed to intra-excitonic resonance,^{12,13} and magnetic-field-induced spin-conserving and spin-flip intersubband transitions.¹⁴

The unusual band lineups of the Al_xGa_{1-x}Sb/InAs/Al_xGa_{1-x}Sb type-II single QW's under ideal condi-

tions with no band bending are schematically depicted in Fig. 1 for three different Al compositions ($x=0, 0.3,$ and 1.0). The effective band gap E_G^* , defined by the energy difference between the lowest electron subband and the highest hole subband, can be varied over a wide range (-0.15 eV $\leq E_G^* \leq +0.3$ eV) by varying x and/or the well width. The end member, GaSb/InAs/GaSb ($x=0$), is a misaligned (or broken-gap) type-II ‘‘semimetallic’’ QW. When the well

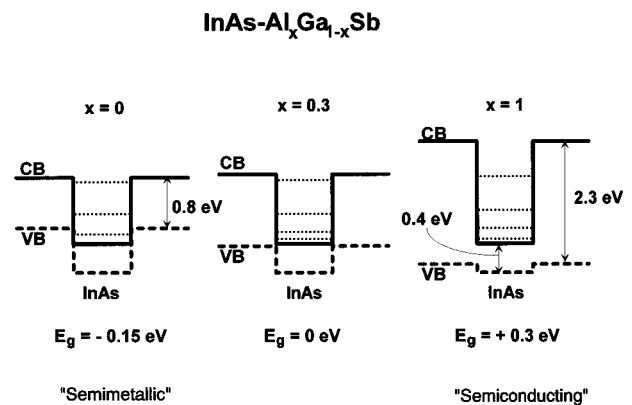


FIG. 1. Schematic conduction (solid lines) and valence (dashed lines) band lineups for InAs-Al_xGa_{1-x}Sb ($x=0, 0.3,$ and 1.0) single quantum wells under ideal conditions (charge transfer and band bending not included). The ideal system is ‘‘semimetallic’’ when $x < 0.3$ (neglecting confinement).

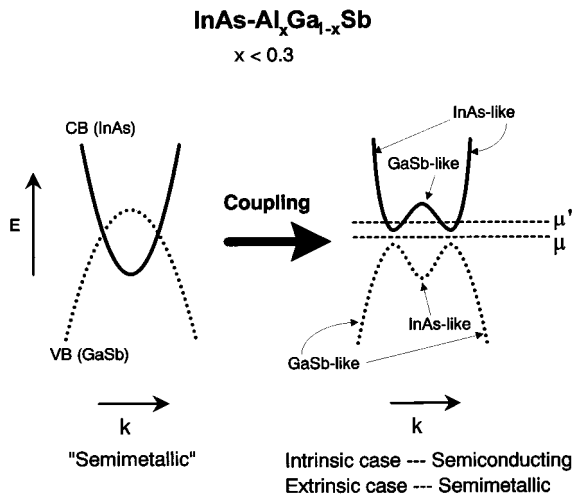


FIG. 2. Schematic in-plane dispersion relations for $\text{InAs-Al}_x\text{Ga}_{1-x}\text{Sb}$ in the “semimetallic” regime ($x < 0.3$), representing the hybridization idea of Altarelli and co-workers (Refs. 15–17). Because of the coupling, an energy gap opens up, making nominally “semimetallic” systems semiconducting if the system is intrinsic (μ). In real systems, because of the existence of defects and/or surface traps that pin the position of the chemical potential (μ'), the system can still be semimetallic.

width is larger than ~ 8 nm, there is a *negative* effective band gap, leading to a charge transfer between the layers, which results in the coexistence of spatially separated *intrinsic* electrons (in InAs) and holes (in GaSb). The overlap between the InAs conduction band and the $\text{Al}_x\text{Ga}_{1-x}\text{Sb}$ valence band decreases with increasing x , vanishing near $x=0.3$, which corresponds to a semimetal-semiconductor transition. In the range $0.3 \leq x \leq 1$, $\text{Al}_x\text{Ga}_{1-x}\text{Sb}/\text{InAs}/\text{Al}_x\text{Ga}_{1-x}\text{Sb}$ is a staggered type-II “semiconducting” QW, in which, although the valence band of $\text{Al}_x\text{Ga}_{1-x}\text{Sb}$ is still higher than that of InAs, there is a positive effective band gap; no intrinsic carriers exist at $T=0$.

Altarelli and co-workers^{15–17} reported interesting results of a series of theoretical investigations on InAs/GaSb type-II broken-gap heterostructures, which are more complex than the above *simple* picture for the “broken-gap” situation. The essential idea¹⁵ on which their calculations are based is that, when $x < 0.3$, the conduction-band states in InAs and the valence-band states in $\text{Al}_x\text{Ga}_{1-x}\text{Sb}$ are resonantly coupled through boundary conditions on the envelope functions at the InAs- $\text{Al}_x\text{Ga}_{1-x}\text{Sb}$ interface, which hybridize the InAs- and $\text{Al}_x\text{Ga}_{1-x}\text{Sb}$ -like in-plane dispersion relations. The coupled in-plane dispersion relations, computed in the framework of the envelope-function approximation, were shown to obey a no-crossing rule which opens up small (a few meV) energy gaps (see Fig. 2). Thus the ideal system is always semiconducting with no mobile carriers at $T=0$, and “semimetallic” behavior observed in many samples with $x < 0.3$ are due to extrinsic effects, which will be discussed in detail in a later section.

In all QW structures fabricated to date, there is always a large density of electrons (10^{11} – 10^{12} cm^{-2}) with high mobilities ($\geq 10^5$ $\text{cm}^2/\text{V s}$) in the InAs wells with no intentional doping. The structures also exhibit an interesting *negative* persistent photoeffect (NPP effect),^{4,5,8} in which illumination at low temperature results in a persistent *decrease* in the

electron density in the well. The origin(s) of the excess electrons in the wells and the NPP effect has been the subject of controversy. Although they have been ascribed to a combination of surface donors in the GaSb cap layers,^{17,18} Tamm-like states at the heterointerfaces,¹⁹ and deep levels (e.g., donors, acceptors, defects, or their complexes) in the $\text{Al}_x\text{Ga}_{1-x}\text{Sb}$ barriers,^{5,8,20,21} the situation is still not completely resolved, and careful studies of controlled samples in which the excess electron density can be varied is necessary to unravel this complex situation.

A large body of theoretical work has been devoted in the last 30 years to electron-hole (e - h) systems in strong magnetic fields, and a fascinating array of possible physical phenomena/states has been predicted—the excitonic insulator phase,²² a gas-liquid-type phase transition,²³ the electron-hole condensate,^{24,25} Bose-Einstein condensation of magnetoexcitons,²⁵ chaos,²⁶ etc. Although much experimental effort has been expended for many years, no direct evidence of these states has been given to date. Attention has been paid to *spatially separated* 2D electrons and holes in layered structures, since the pioneering work of Lozovik and co-workers,²⁷ who considered the pairing of electrons and holes across an interface of two-media, and the superfluidity of such pairs. A very interesting but complicated many-particle situation arises, especially in the presence of strong perpendicular magnetic fields. In such a situation, spatially separated 2D electrons and holes, both Landau quantized, are present, and there is a Coulomb attraction between them as well as electron-electron (e - e) and hole-hole (h - h) correlations. Several authors have investigated this situation theoretically,^{28–31} suggesting a number of interesting possibilities. Various types of semiconductor heterostructure systems to realize this situation experimentally have been recently proposed and/or fabricated.^{32–34} Both optical measurements^{35,36} and transport measurements³⁷ on such structures have exhibited interesting effects, rekindling interest in this fundamental problem.

Cyclotron resonance has been a powerful tool for studying the basic properties of carriers in solids, and has been applied to many quasi-2D systems over the past two decades.³⁸ However, important aspects of 2D CR still remain unresolved and controversial. Apparently contradictory results for the CR of electrons in narrow (~ 10 – 20 nm) InAs QW’s have been reported.^{10,11,39} For an InAs/GaSb QW, Heitman, Ziesmann, and Chang³⁹ observed pronounced oscillations in CR amplitude and linewidth (but not mass) with filling factor $\nu = n_s h/eB$, where n_s is the 2D carrier density—similar to, but much stronger than, those observed by Englert *et al.* in a GaAs/ $\text{Al}_x\text{Ga}_{1-x}\text{As}$ heterostructure.⁴⁰ Linewidth maxima were observed at *even* ν ’s and minima at *odd* ν ’s. While the authors attributed the oscillations to ν -dependent screening of impurity scatterers by the 2D electron gas,⁴¹ it remains an unsettled question as to why this particular 2D system shows such pronounced oscillations. More recently, two groups^{10,11} observed spin-resolved CR in *InAs/AlSb* QW’s. Their data clearly reveal linewidth maxima (or larger splittings) at *odd* ν ’s, inconsistent with Ref. 39 but consistent with the idea⁴² that the onset of unresolved CR splittings due to nonparabolicity is the cause of oscillations. The primary difference between the earlier³⁹ and later^{10,11} experiments is the barrier material: GaSb or AlSb, respectively. Thus InAs

QW's with $\text{Al}_x\text{Ga}_{1-x}\text{Sb}$ barriers with variable composition (x) comprise an ideal system to elucidate this point.

In this paper we present results of detailed and systematic FIR magneto-optical studies on a series of high-mobility InAs/ $\text{Al}_x\text{Ga}_{1-x}\text{Sb}$ single QW samples with $x=1.0, 0.8, 0.5, 0.4, 0.2,$ and 0.1 . This is an extension of our earlier work on these samples, which has revealed several phenomena.^{12,13} For semiconducting samples ($x \geq 0.4$), we observed spin-resolved CR, similar to the results of other groups^{10,11} on InAs/AlSb QW's. For semimetallic samples ($x=0.1$ and 0.2), we observed additional FIR lines (X lines) *only when* there is substantial band overlap between "barrier" and "well" materials *and* low enough chemical potential at low enough temperatures and high enough magnetic fields.¹³ We ascribed the X lines to excitonic resonances [$1s \rightarrow 2p_{\pm}$ in the low-field hydrogenic notation, and $(N=0, M=0) \rightarrow (N=1, M=1)$ in the high-field notation, where N is the Landau quantum number and M is the quantum number for the z component of the angular momentum]; the excitons are composed of spatially separated electrons and holes. In addition, we observed very strong oscillations in the CR linewidth, amplitude, and mass which correlate approximately with the Landau-level filling factor in semimetallic samples.¹² Maximum linewidths, minimum amplitudes, and mass jumps were observed at *even*-integer filling factors, so that unresolved nonparabolicity-induced CR splitting⁴² is *not* the cause of the oscillations. The strength of the oscillations increased with e - h pair density; the oscillations were *not* observed for any of the semiconducting samples ($x \geq 0.4$) in which only electrons exist. The strength also depended sensitively on temperature, decreasing with increasing temperature, and all oscillations disappeared at high enough temperatures (>50 K), where e - h interaction becomes relatively unimportant. Results thus strongly indicate that filling-factor-dependent Coulomb interaction between electrons and holes plays a significant role in the origin of the strong oscillations. Furthermore, detailed studies on the semimetallic sample with an optically pumped FIR laser have revealed several lines. Our studies showed that structures in laser spectroscopy and some aspects of CR previously observed in Fourier-transform spectroscopy,^{12,13} result at least in part, from band-structure effects. That is, the hole states in the $\text{Al}_x\text{Ga}_{1-x}\text{Sb}$ barriers are coupled to the electron states in the InAs wells. This leads to a unique band structure in a magnetic field, and FIR lines whose transition energy goes to zero at finite magnetic field but rapidly become CR-like transitions with increasing magnetic field, qualitatively consistent with the theory of Fasolino and Altarelli.¹⁶

II. SAMPLES AND EXPERIMENTAL METHODS

The six samples investigated in the present work were grown by molecular-beam epitaxy under the same growth conditions. Only the Al composition x of the $\text{Al}_x\text{Ga}_{1-x}\text{Sb}$ barrier layers was varied: $x=1.0, 0.8, 0.5, 0.4, 0.2,$ and 0.1 . The nominal sample structure consisted of a 15-nm InAs QW sandwiched between two $\text{Al}_x\text{Ga}_{1-x}\text{Sb}$ barrier layers grown on a semi-insulating GaAs substrate, with thicknesses of the upper and lower barrier of 15 nm and 3 μm , respectively. A 10-nm GaSb cap layer was grown on top of the entire structure. Samples were not intentionally doped, but a

TABLE I. The electron densities and mobilities of the samples studied. The numbers in parentheses are the values after LED illumination. Densities were obtained at 4.2 K and mobilities at 77 K.

No.	x	Density (10^{11} cm^{-2})	Mobility ($10^5 \text{ cm}^2/\text{V s}$)
1	1.0	9.5 (6.0)	0.3
2	0.8	8.2 (5.0)	0.5
3	0.5	8.5 (6.1)	2.2
4	0.4	6.4 (5.4)	0.9
5	0.2	6.4 (5.8)	1.7
6	0.1	6.2 (5.5)	1.1

large density of free electrons was found in the InAs wells; the carrier densities and mobilities deduced from magnetotransport measurements performed on the same set of samples⁸ are listed in Table I. The 2D hole densities at zero field after illumination were estimated to be $\sim 1\text{--}2 \times 10^{11} \text{ cm}^{-2}$ for sample 6 from high-temperature cyclotron-resonance (CR) intensities, and $\sim 0.3 \times 10^{11} \text{ cm}^{-2}$ for sample 5 from magnetotransport measurements.⁸

All the samples showed the NPP effect,^{4,5,8} which was used to reduce electron densities in the well [and to increase hole densities in the barrier(s) for semimetallic samples]; to induce this effect a red light-emitting diode (LED) was mounted *in situ*. Fourier-transform spectrometers and an optically-pumped FIR molecular-gas laser were used in conjunction with 9- and 17-T superconducting magnets and a 23-T Bitter-type magnet to carry out the FIR magnetospectroscopy on these samples. A Si composite bolometer and photoconductive Ge:Ga and Si:B detectors were used to cover the whole spectral range of interest 10–500 cm^{-1} . Light pipes, a reflecting mirror, and condensing cones were used to guide FIR light from the spectrometer to the sample/detector. For circular polarization measurements with the FIR laser, a $\lambda/4$ plate, made of x -cut single-crystal quartz, in conjunction with a linear polarizer, is placed in front of the sample. Different $\lambda/4$ plates with different thicknesses were prepared for different FIR wavelengths.

III. EXPERIMENTAL RESULTS

A. Semiconducting samples: $x=1.0, 0.8, 0.5,$ and 0.4

Samples 1–4 ($x=1.0, 0.8, 0.5,$ and 0.4) have positive effective band gaps, and thus show semiconducting behavior both in magnetotransport⁸ and magneto-optical^{12,13} properties. No holes exist in these samples, excess 2D electrons in the InAs being the only carriers. In Fig. 3 typical transmittance spectra (ratioed to a zero-field spectrum) for sample 3 ($x=0.5$) at several magnetic fields are displayed in the energy range 80–200 cm^{-1} . A sharp absorption feature (transmission minimum) due to the CR of 2D electrons in the InAs well is the only spectroscopic feature in this energy range. Because of the large nonparabolicity of the conduction band in InAs and the high mobility of the participating 2D electrons, CR splittings are clearly observed. These splittings come from the energy dependence of the effective mass and the effective g factor of the electrons (alternatively, from the nonuniform spacing of the Landau and spin levels). The dominant low-energy [high-energy] line of the resolved two

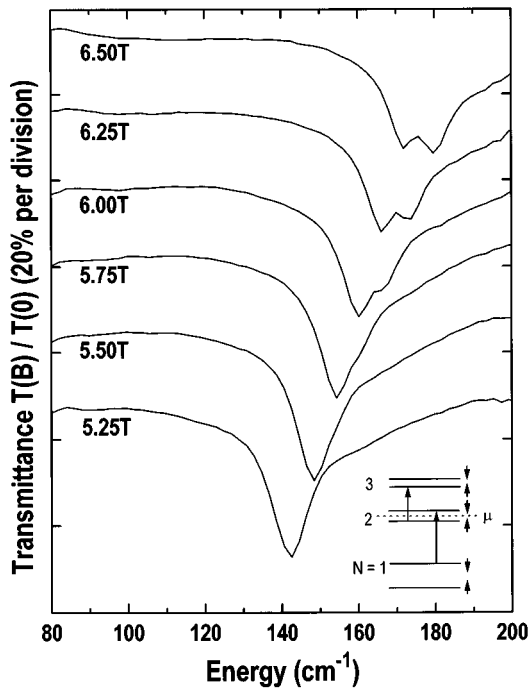


FIG. 3. Transmittance spectra (ratioed to a zero-field spectrum) for sample 3 ($x=0.5$; semiconducting) at 4.2 K before LED illumination at several magnetic fields. Splittings are due to the energy dependence of effective mass and g factor, as shown schematically in the inset, arising from the large nonparabolicity of the InAs conduction band.

lines in Fig. 3 corresponds to the transition $(2, \uparrow) \rightarrow (3, \uparrow)$ [$(1, \downarrow) \rightarrow (2, \downarrow)$], where the numbers are Landau indices, and \uparrow and \downarrow denote the parallel and antiparallel spin projection, as shown in the inset.

Illumination always reduced the CR integrated intensity and increased the transition energy (i.e., the cyclotron energy, $\hbar\omega_c = \hbar eB/m^*$). The CR integrated intensity, which is proportional to the 2D electron density, was reduced by about 28%, while the transition energy was shifted to higher energy (lighter effective mass) by about 4 cm^{-1} after illumination. Both the decrease in intensity and the position shift are consistent with the single-particle picture; the Fermi energy E_F (or the electron density) of the system is lowered by illumination as a result of the NPP effect,^{4,5,8} and the CR mass is reduced due to the nonparabolicity of the InAs conduction band [the lower E_F , the lighter the mass, or, alternatively, in the high-field region (inset to Fig. 3) the transitions have larger contributions from lower (more widely separated) Landau levels]. When we tilted the magnetic field from the normal to the sample surface, the resonance position shifted down following the cosine rule, indicating the strongly 2D nature of the electrons participating in CR.

All the other semiconducting samples ($x=1.0, 0.8$, and 0.4) showed similar behavior to sample 3, which can be understood predominantly in terms of single-particle band-structure effects. No evidence of electron-LO-phonon resonant coupling was found around the InAs reststrahlen band, $219\text{--}243 \text{ cm}^{-1}$, although a dielectric effect at the TO-phonon energy, similar to the results reported for an InAs/GaSb QW,⁴³ was observed. We believe that screening effects⁴⁴ and

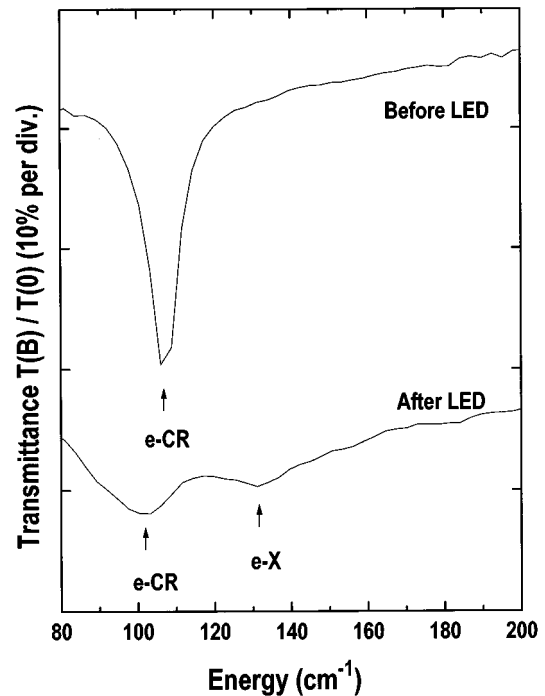


FIG. 4. Transmittance spectra for sample 5 ($x=0.2$) at 4 T before and after exposure to a red LED. Illumination results in a dramatic change: CR frequency decreases, opposite to the expectation from nonparabolicity, and a line, referred to as the e -X line in this paper, appears above CR.

occupation effects⁴⁵ due to the large electron density in the samples play a crucial role in reducing the coupling. An attempt to reduce the electron density without reducing the mobility by gating the sample is in progress.

B. Intermediate sample: $x=0.2$

In sample 5 ($x=0.2$) there is small overlap ($\sim 50 \text{ meV}$) between the bulk conduction band of InAs and the bulk valence band of $\text{Al}_{0.2}\text{Ga}_{0.8}\text{Sb}$. In the simple picture described earlier (Fig. 1), the characteristic behavior of this sample can be qualitatively understood in terms of the position of the Fermi energy E_F . Before LED illumination at low temperature, E_F at zero field in this sample is such that $E_1 + E_F$ (measured from the bottom of the InAs conduction band), where E_1 is the confinement energy for the lowest electron subband, is slightly lower than the highest hole subband-edge at the interface(s); hence a small density of 2D holes can exist on the $\text{Al}_{0.2}\text{Ga}_{0.8}\text{Sb}$ side of the interface(s), and so the system is slightly “semimetallic.” Applying a modest magnetic field (a few T) depopulates the holes and transforms the system into a semiconductor in which only electrons exist. LED illumination lowers E_F due to the NPP effect, decreasing the electron density and increasing the hole density, making the system more strongly “semimetallic;” hence the field at which holes vanish moves up to about $7\text{--}8 \text{ T}$.⁸

The above picture is consistent with most aspects of FIR spectra obtained, although a few details cannot be explained without invoking the “antiparabolicity” arising from the hybridization of electron and hole Landau levels across the interface (see Fig. 2). In Fig. 4 two transmittance traces are

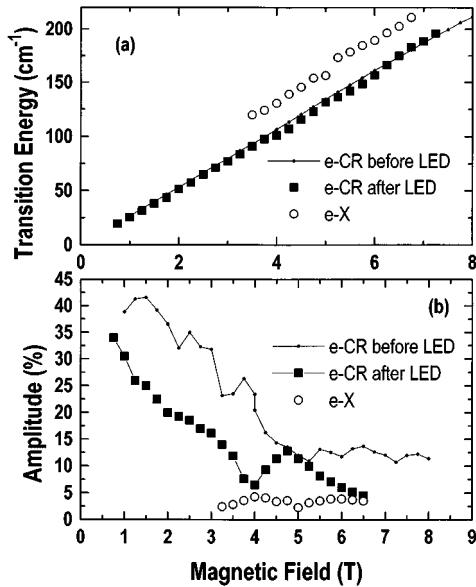


FIG. 5. (a) Transition energy vs field for CR and the e -X line observed for sample 5 ($x=0.2$) at 4.2 K. (b) Peak absorption amplitude vs field. Dramatic reduction ($\sim 30\%$) in intensity due to magnetic-field-induced semimetal-semiconductor transition can be seen. Oscillatory behavior is seen for both lines at high fields (>3 T) after LED illumination.

shown for sample 5 at 4 T before and after LED illumination, respectively. A single sharp CR line is observed before illumination, similar to that observed for semiconducting samples, since before illumination the system at this field is expected to be semiconducting from the above considerations. After illumination CR shifts *down* in energy and broadens substantially; in addition, an interesting feature, referred to as the e -X line in this paper, appears 30 cm^{-1} above CR. The appearance of the e -X line indicates that the system is “semimetallic;” this line is absent in all the semiconducting samples, but is more clearly observed in sample 6, which is the most strongly “semimetallic.” The decrease in energy for CR is *not* expected from the usual band nonparabolicity, for which CR should shift *up* after LED illumination.

A plot of transition energy against field in Fig. 5(a) for CR before LED illumination exhibits a nearly linear dependence, corresponding to a mass of $0.035m_0$ at the Fermi energy, much higher than the band-edge mass ($0.024m_0$) due to nonparabolicity. As shown in Fig. 5(b), this line *decreases* in amplitude monotonically with increasing magnetic field in the field range ~ 1.5 to ~ 5 T, consistent with the above-mentioned field-induced e - h depopulation. Above 4 T, CR intensity remains constant with field, since there are no holes and only excess electrons exist for $B > 4$ T. From the CR integrated intensity, we obtained for 2D electrons $n_s \approx 7 \times 10^{11}\text{ cm}^{-2}$ for $B < 2$ T and $n_s \approx 4 \times 10^{11}\text{ cm}^{-2}$ for $B > 4$ T, deducing a zero-field hole density of $\sim 3 \times 10^{11}\text{ cm}^{-2}$. This number is considerably larger than the value obtained from magnetotransport measurements;⁸ in a later section we show that this is also due to the hybridization (see Fig. 2), which modifies the simple relation between the CR integrated intensity and the electron density.

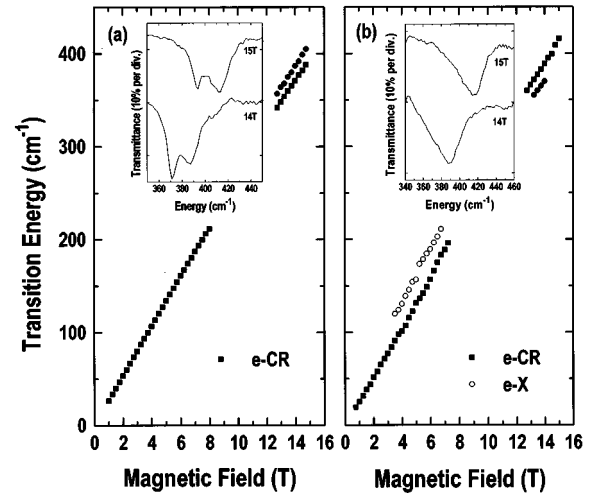


FIG. 6. High-field (11–15 T) behavior of sample 5 ($x=0.2$): (a) before and (b) after LED illumination. The insets show typical transmittance spectra at 4.2 K. Nonparabolicity-induced CR splittings can be seen, similar to the results for semiconducting samples (see Fig. 3).

In Fig. 5 we also show (a) transition energy vs field and (b) peak absorption amplitude for both CR and the e -X line *after* LED illumination. At low magnetic fields (< 4 T), we observe a single sharp line due to e -CR, similar to the e -CR line observed before illumination but with smaller intensity and larger linewidth (see Fig. 4). In the field range 1–4 T, e -CR loses intensity rapidly with increasing field—qualitatively the same behavior as before illumination. However, at about 4 T, where there is still a large density of holes, the e -X line begins to be observed about 30 cm^{-1} above e -CR. The transition energy vs field for both lines shows slight deviation from straight lines [see Fig. 5(a)]. e -CR exhibits an *average* linear dependence on B , extrapolating to zero at zero field, whereas the e -X line extrapolates to a finite energy ($\sim 25\text{ cm}^{-1}$) at zero field. We assign the e -X line to an internal transition ($1s \rightarrow 2p_+$ -like) of excitons composed of spatially separated electrons and holes. This line is observable only at temperatures < 40 K and magnetic fields > 4 T, consistent with the notion that applied perpendicular fields stabilize the quasi-2D excitonic state by shrinking the e - h wave function in the 2D plane. More details of the behavior of the e -X line and discussion of its origin in terms of an excitonic ground state are given in Sec. IV.

Figure 6 shows the high-magnetic-field behavior (up to 15 T) of sample 5. A Si:B photoconductive detector was used to cover the energy range of interest, 300 – 500 cm^{-1} . There is a gap region between 220 and 320 cm^{-1} , where transmission experiments were impossible because of the reststrahlen band of the GaAs substrates. Before illumination (a), a sharp e -CR remains the only feature, but shows splittings due to nonparabolicity. These splittings are of the same origin as those observed for semiconducting samples (see Sec. III A), consistent with the fact that sample 5 is completely semiconducting (i.e., there are no holes) in this high-field range. After illumination (b), we observe an asymmetric broad feature consisting of two CR lines, for which peak positions were deduced from line-shape analysis. We believe that these two lines arise from the nonparabolicity-induced splitting, as be-

fore illumination, but they are not resolved because of line broadening. The line-broadening due to illumination is consistent with illumination-induced mobility reduction observed in similar systems (see, e.g., Refs. 4 and 5), but its microscopic origin is still elusive as is the origin of the electron accumulation and the NPP effect. The possibility that the high-energy line in Fig. 6(b) is the e - X line can be ruled out, since the transition energies of the two lines are nearly identical to those of the two lines observed before illumination in the same field range [Fig. 6(a)] and the separation between the two lines ($\sim 15 \text{ cm}^{-1}$) is only half that of the e - X - e -CR separation (30 cm^{-1}). Therefore, we conclude from Fig. 6(b) that the e - X line is already gone at $B > 12 \text{ T}$ after illumination. This is also evidence that the e - X line arises from e - h interaction, since in this field range no holes are available.⁸

C. A semimetallic sample: $x=0.1$

1. Illumination and field dependence of e -CR and e - X

Sample 6 ($x=0.1$) is more strongly “semimetallic,” having larger band overlap, than sample 5 ($x=0.2$). In the simple picture in which hybridization between electron states and hole states is not considered, the 2D electrons are confined in the 15-nm InAs well, and the 2D holes are confined at the heterointerface(s) by self-consistent band-bending resulting from charge transfer.⁴⁶ The position of E_F is always between the lowest electron subband edge and the highest hole subband edge, so that both electrons and holes exist. Illumination lowers E_F , increasing the hole density and decreasing the electron density. Therefore, the e - X line, observed *only* after illumination in a certain field range for sample 5, is observable for sample 6 at fields above $\sim 1 \text{ T}$, both before and after illumination, with increased intensity after illumination. When the illumination time reaches about 500 ms, the e - X line becomes comparable in intensity to e -CR in intensity, finally becoming the dominant line at the highest photon dose. It should be noted that, compared to the *positive* persistent photoeffect commonly observed in GaAs-Al _{x} Ga _{$1-x$} As QW structures, the time constant is extremely long, consistent with magnetotransport experiments.^{5,8}

The typical magnetic-field dependence of transmittance spectra at 4.2 K for sample 6 is shown in Fig. 7 for field regimes 1.0–3.0 T [in (a)] and 3.5–7.0 T [in (b)]. In the low-field regime $B < 2.5 \text{ T}$, e -CR is dominant and sharp. With increasing field, however, the e - X line increases in intensity very rapidly at the expense of e -CR, suggesting that perpendicular magnetic fields stabilize the quasi-2D excitonic state. In the field range 3–7 T, the intensities of both lines oscillate with field in such a way that e -CR maxima coincide approximately with minima of the e - X line, and vice versa. Both the linewidth and amplitude of e -CR also oscillate strongly, linewidth maxima and amplitude minima occurring simultaneously in the vicinity of even ν 's (e.g., at $B=5.5$ – 6.0 T , corresponding to $\nu \sim 4$) [12].

In Fig. 8 we plot transition energy [in (a)] and percent peak absorption amplitude [in (b)] against magnetic field up to 7.5 T after illumination at 4.2 K for both e -CR and e - X , along with another, low-frequency line, referred to as the h - X line in this paper. Details of the h - X line are given in

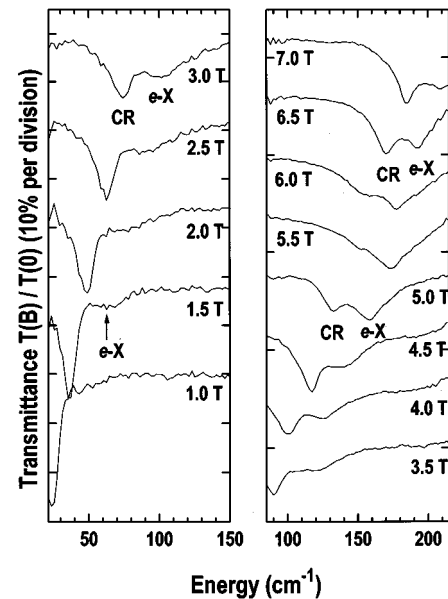


FIG. 7. Transmittance spectra for sample 6 ($x=0.1$; semimetallic) at 4.2 K after LED illumination in field ranges (a) 1.0–3.0 T and (b) 3.5–7.0 T. A single sharp CR is seen in low fields, but it loses strength rapidly with increasing field and a new peak (e - X line) appears at high fields, similar to sample 5 ($x=0.2$) after LED illumination.

Sec. III C 3. The straight line in Fig. 8(a) has an effective mass of $m^*=0.0352m_0$, which we call “the high-temperature mass,” as we discuss later (Sec. III C 3). Open diamonds are data obtained with a FIR laser, and will be discussed in Sec. III C 5. We observe an anomalous “anti-

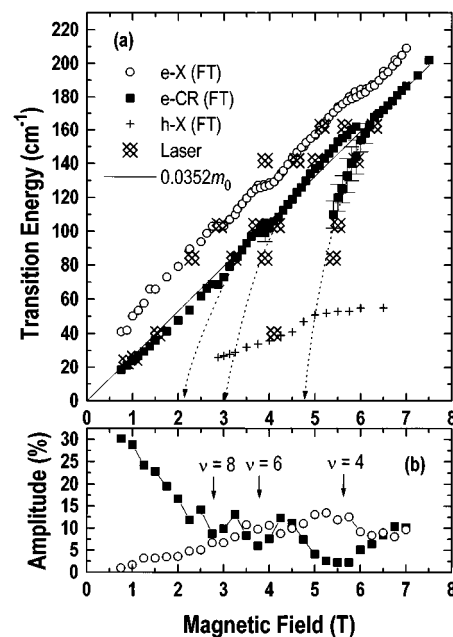


FIG. 8. Sample 6 ($x=0.1$; semimetallic) after exposure to a LED. (a) Transition energy vs magnetic field for e -CR, e - X line, and h - X line at 4.2 K, including both Fourier transform (FT) and laser spectroscopy, along with a straight line that corresponds to a mass of $0.0352m_0$. (b) Plot of percent change in transmittance at peak vs magnetic field for e -CR and the e - X line.

nonparabolic'' field dependence of the transition energies for both e -CR and e -X in Fig. 8(a): (1) they show large slope discontinuities at fields near 3, 4, and 6 T (corresponding approximately to $\nu=8, 6,$ and $4,$ respectively); (2) the cyclotron mass ($m_{\text{CR}}^* = eB/\omega_{\text{res}}$) is found to *decrease* monotonically with increasing field between two adjacent discontinuities; (3) the transition energy jumps *down* with increasing field at each discontinuity (i.e., the transition energy just before a discontinuity is *higher* than the transition energy just after that discontinuity); (4) there are at least three CR branches whose transition energies extrapolate to zero at finite magnetic field (see also Sec. III C 5). None of these observations is expected from the usual band nonparabolicity, for which the mass should *increase* with field and the transition energy should jump *up* at integers ν .^{10,11} Despite these anomalies, both lines show an *overall* linear dependence on field with *essentially the same average slope* ($\sim 0.035m_0$). The equivalence of the slopes strongly suggests that the e -X line is associated with 2D electrons in the InAs well. The amplitude of the e -X line increases rapidly with magnetic field at the expense of e -CR in the low-field region ($B < 3$ T), as shown in Fig. 8(b), qualitatively the same behavior as sample 5 after illumination. However, at higher fields it oscillates strongly, with maxima coincident with the minima in the e -CR intensity near even ν 's. All the above results suggest the importance of the filling factor in determining intensity, position, and linewidth both for e -CR and the e -X line.

2. CR oscillations with filling factor

In the magnetic-field dependence of e -CR for samples 5 and 6, we have observed strong oscillations in mass, amplitude, and linewidth. We found that these oscillations are observable only in the "semimetallic" situation at low enough temperatures and high enough magnetic fields, and that they appear to be correlated with filling factor ν . In Fig. 9 we plot e -CR mass, amplitude, and linewidth against ν for sample 6 ($x=0.1$) at 4.2 K after LED illumination. It can be clearly seen in Fig. 9(a) that the CR mass oscillates strongly, with abrupt mass changes at even-integer ν 's. As noted before, between two adjacent even integer ν 's (e.g., $\nu=6$ and 4), the CR mass *decreases* with decreasing ν (increasing B), opposite to what would be expected from nonparabolicity. The ν -dependent oscillations in amplitude and linewidth [Figs. 9(b) and 9(c)] are similar to earlier results for InAs/GaSb QW's.³⁹ Pronounced oscillations are seen, linewidth maxima and amplitude minima occurring at *even*-integer ν 's;⁹ dramatic line broadening with concomitant amplitude reduction is observed at $\nu=4$. Thus the onset of nonparabolicity-induced CR splittings⁴² is *not* the cause of the oscillations, since it predicts linewidth maxima at *odd*-integer ν .

Another important experimental finding is that the strength of the CR oscillations increases with increasing e - h pair density (or decreasing Fermi energy) (see Ref. 12 for details). As we described in Sec. III B, before illumination for sample 5, only e -CR, which does *not* exhibit oscillations, is observed. After illumination for sample 5, both e -CR and the e -X-line are observed, *and* CR mass, amplitude, and linewidth oscillate. Sample 6 before illumination shows stronger oscillations than sample 5 after illumination, reflecting the fact that sample 6 always has a higher e - h pair den-

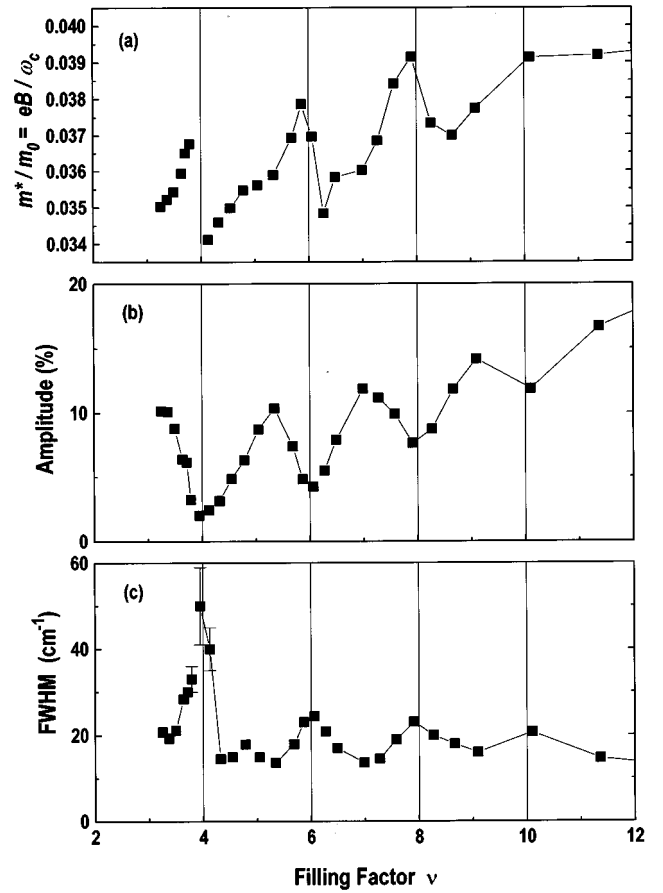


FIG. 9. Electron CR oscillations vs filling factor for sample 6 after illumination at 4.2 K: (a) percent absorption amplitude and (b) full width at half maximum. Values were obtained from fits of Lorentzians to the data.

sity than sample 5; after illumination it shows even stronger oscillations. The strength of the amplitude and linewidth oscillations and the intensity of the e -X line show qualitatively the same behavior, i.e., they also increased with increasing e - h pair density (or decreasing E_F), indicating that the oscillations and the emergence of the e -X line are correlated.

Finally, as we describe in Sec. III C 3, the strength of all the oscillations and the intensity of the e -X line become weaker with increasing temperature, and disappear at high enough temperatures ($T > 50$ K). In other words, all the anomalies observed for sample 6 are possible only at low enough temperature. This also strongly supports the idea that all the oscillations and the e -X line are related to e - h Coulomb interaction (and the density of holes), which become relatively unimportant at high temperatures.

3. Temperature dependence

Temperature dependence was studied in detail in sample 6 at several magnetic fields. Figure 10(a) shows transmittance spectra for this sample at $B=5$ T ($\nu=4.6$) and at several different temperatures. At $T=4.2$ K, the e -X line at 160 cm^{-1} dominates the spectrum. With increasing temperature, however, e -CR increases in intensity rapidly while e -X decreases. Above 20 K, e -CR becomes dominant over e -X, and above 50 K e -X is a weak shoulder on the high-energy side

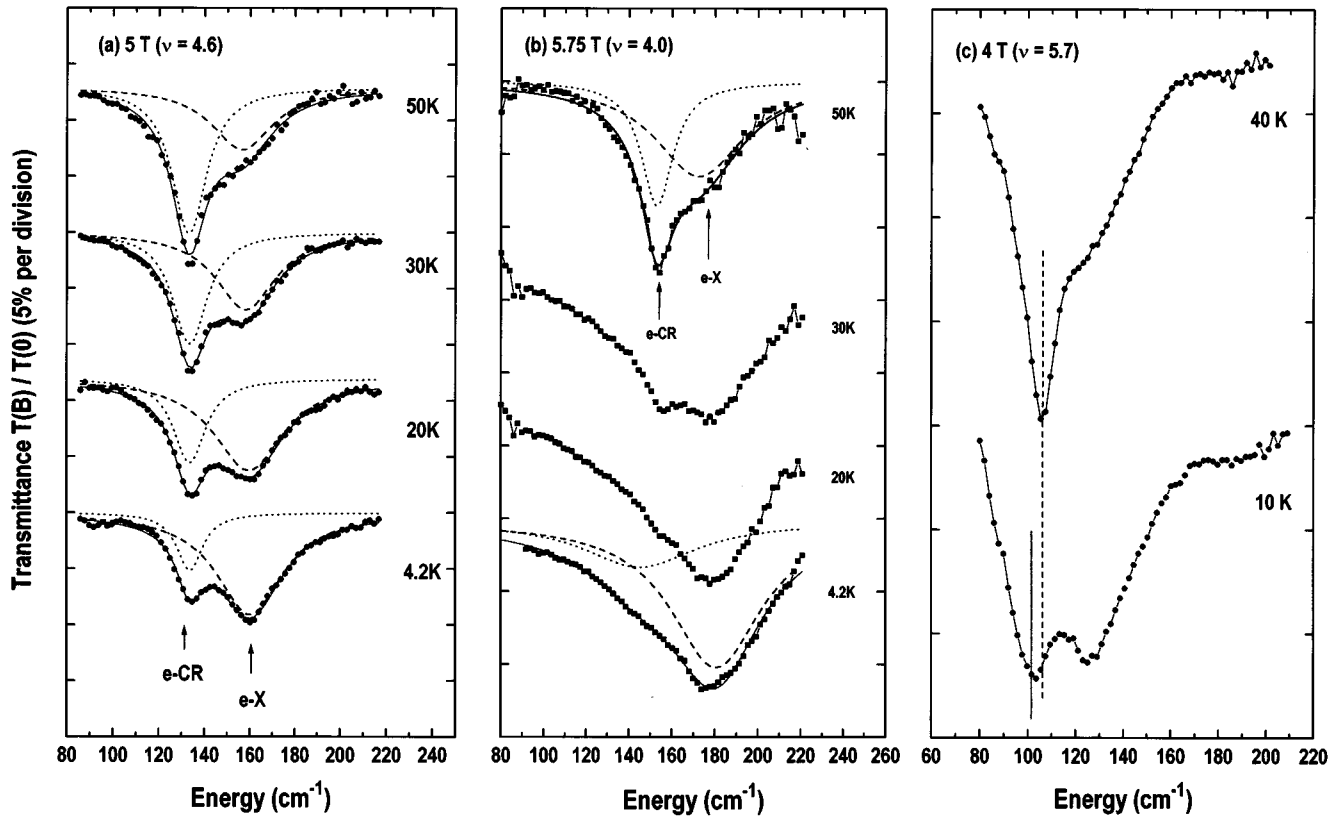


FIG. 10. Temperature dependence of e -CR and the e -X line for sample 6 after exposure to the LED. Ratios of transmitted intensity at the indicated temperature to a background spectrum (at the same temperature and $B=0$) are shown by the solid circles. Individual Lorentzian lines fitted to the data—dotted lines for e -CR and dashed lines for the e -X line; overall fit—solid lines. (a) $B=5$ T, (b) $B=5.75$ T, and (c) $B=4$ T. In (c) it is clearly seen that with increasing temperature the CR frequency shifts up, the CR strength increases, and the CR line becomes narrower.

of e -CR. The spectra can be fitted very well by two Lorentzians, as indicated in the figure. The clear decrease in the intensity of the e -X line at higher temperatures suggests that it is associated with a bound state—an excitonic state in this case. Note also that e -X is always broader than e -CR, indicative of a basically different origin. At other magnetic fields, the general temperature dependence is the same, in the sense that e -CR increases and e -X decreases with temperature, but details are sometimes very different, with the filling factor being an important quantity. Especially at fields close to even integers ν , as shown in Fig. 10(b) for the case of $B=5.75$ T ($\nu \sim 4$), higher temperatures were required for e -CR to become dominant. This behavior is consistent, with the e - h interaction (and consequently the excitonic binding energy) being larger at even ν 's than at odd ν 's.

It was also found that the CR mass, amplitude, and linewidth change considerably with temperature. Figure 10(c) shows two spectra for sample 6 at 4 T ($\nu=5.7$) obtained at 40 and 4.2 K, respectively. It can clearly be seen that at 40 K the CR frequency is higher, the CR amplitude is larger, and the CR linewidth is narrower, than the corresponding quantities at 4.2 K. In Fig. 8(a) we indicated a straight line having an effective mass of $m=0.0352m_0$, which we call “the high-temperature mass:” the CR mass always approaches this mass when temperature is raised at any magnetic field. In Fig. 11 we plot the measured CR frequencies, in terms of the shift from the position expected for the high-temperature

mass, as a function of temperature T between 4.2 and 70 K for several magnetic fields (filling factors) for sample 6. The data point at 5.75 T ($\nu=3.95$) and 4.2 K is omitted because of the large uncertainty in the position of the very weak and broad peak. It is clearly seen in the figure that the energy shift always approaches zero at any ν as temperature is raised; i.e., if the energy shift at low temperature is positive

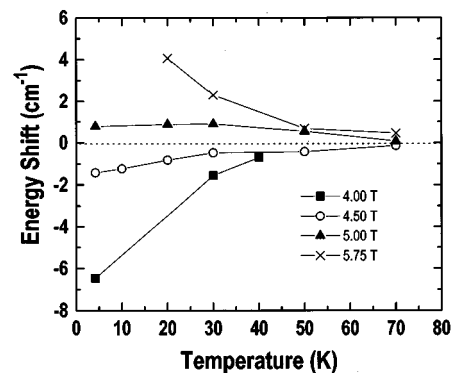


FIG. 11. The temperature dependence of CR position at four different fields (filling factors). The abscissa measures the energy shift from the energy expected from the high-temperature mass [$0.0352m_0$, see the straight line in Fig. 8(a)]. No data points at 5.75 T and 4.2 K is included because of the very large uncertainty in resonance position.

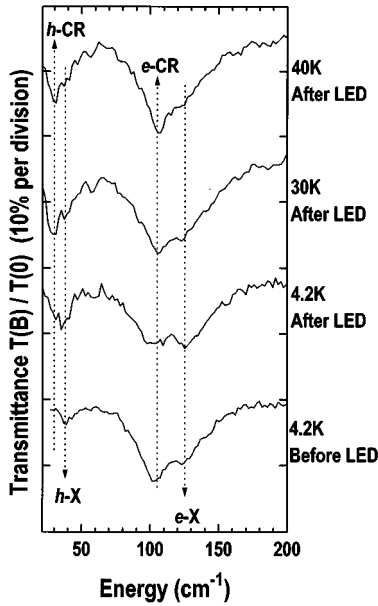


FIG. 12. Transmittance spectra for sample 6 under different temperature and illumination conditions. Two electronlike lines and two hole like lines are clearly observed.

(negative), it decreases (increases) with increasing temperature. In short, at high enough temperatures, the discontinuities in transition energy vs field, seen in Fig. 8(a), disappear, and the transition energy shows the usual linear dependence on B . Similar tendencies are seen for amplitude and linewidth as well. Therefore, it can be concluded that all the oscillations become less pronounced with increasing temperature, disappearing at high enough temperatures ($T > 50$ K), and the mass, amplitude, and linewidth of e -CR approach their mean values between maxima and minima. At high temperatures, e - X also disappears—again consistent with the notion that the oscillations are intimately related to e - h correlations.

We have observed two other lines, h -CR and the h - X line, that arise from holes in the $\text{Al}_{0.1}\text{Ga}_{0.9}\text{Sb}$ barriers, in a lower-frequency region, as shown in Fig. 12. Transition energy vs field for the h - X line can be found in Fig. 8(a). Figure 12 displays FIR spectra in the energy range 30–200 cm^{-1} for sample 6 at 4 T for several temperatures and under different illumination conditions. There are four distinct features in this spectral range. The line at 125 cm^{-1} is the e - X line, and the line at 105 cm^{-1} is e -CR, as before. The e - X line increases in intensity with decreasing temperature and/or increasing hole (or electron-hole pair) density at the expense of e -CR intensity, consistent with the idea of e - h binding. Its intensity is larger after LED illumination than before illumination since illumination increases electron-hole pair density. Qualitatively the same behavior can be seen for the h - X line (at 40 cm^{-1}) and h -CR: the h - X line increases in intensity with decreasing temperature and/or increasing electron-hole density at the expense of h -CR intensity. At the highest temperature, only e -CR and h -CR are observable, consistent with the notion that electrons and holes are thermally liberated from bound states. The fact that h -CR is not observed at low temperatures leads us to conclude that *all the holes are bound at low temperatures in the form of excitons*.

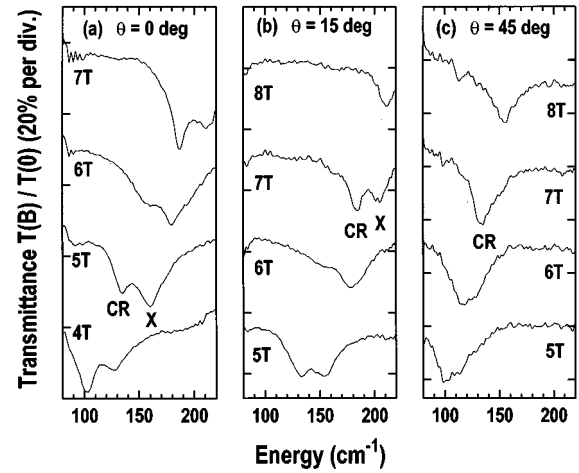


FIG. 13. Transmittance spectra for sample 6 ($x=0.1$; semimetallic) at several magnetic fields and at different angles of the field with respect to the normal to the sample surface: (a) 0° , (b) 15° , and (c) 45° .

4. Tilted-field experiments

Interesting aspects of the e - X -line were found when we tilted the magnetic field with respect to the growth axis. Both e -CR and e - X shifted down in energy with a small tilt angle, indicating that they are 2D in nature. However, e - X was found to lose intensity rapidly with increasing tilt angle, while the CR intensity was maintained and the CR position followed the cosine dependence on angle typical of 2D confinement.

Figure 13(a) displays typical transmittance spectra at several magnetic fields, between 4 and 7 T, with the magnetic field normal to the sample surface for sample 6 ($x=0.1$). At 4 T CR is dominant, but it rapidly loses intensity and broadens with increasing field, and becomes a shoulder on the e - X -line at 6 T. However, CR regains intensity with further increasing field, and quickly becomes dominant again at 7 T. This general behavior can be also seen at a 15° tilt angle [Fig. 13(b)], but with slightly different line shape and reduced frequencies both for CR and e - X , indicating the 2D nature of both lines. If we take the normal component of B ($B \cos 15^\circ$) in Fig. 13(b), and compare the spectra with those taken with B at normal incidence in Fig. 13(a), we notice that not only the frequencies but also the relative intensities of the two lines correspond almost exactly. However, at 45° , as shown in Fig. 13(c), e - X dramatically shifts down in energy and loses intensity, while e -CR shifts down in energy as the cosine of the angle between the field and surface normal, and increases in intensity. At 7 and 8 T, e - X is not detectable.

These results suggest that a large in-plane magnetic field tends to destroy e - X in favor of e -CR, in contrast to a large perpendicular magnetic field, which stabilizes it. We believe that this effect is consistent with other experimental observations, and can be explained as follows. As we have seen, all the observed anomalies, including the appearance of e - X , are correlated with the e - h pair density (or the overlap between the InAs conduction band and the $\text{Al}_x\text{Ga}_{1-x}\text{Sb}$ valence band)—the e - X line increases in intensity with increasing e - h pair density at the cost of e -CR intensity. When a magnetic field is applied parallel to the 2D plane ($\mathbf{B} \parallel y$, where z is the growth axis), electrons moving in the positive and nega-

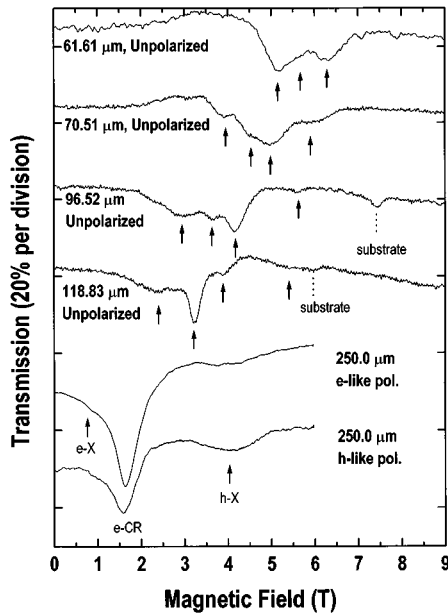


FIG. 14. FIR laser transmission spectra for sample 6 ($x=0.1$; semimetallic) at five different wavelengths. The data were taken with unpolarized FIR radiation, except for the lower two traces, for which circularly polarized FIR light at $250 \mu\text{m}$ was used. High-field lines observed in the middle two traces are bulk CR in GaAs. In the lower two traces it can be clearly seen that the e - X line and e -CR are electronlike and the h - X -line is holelike.

tive x directions are affected by different Lorentz forces, and the subband structure is modified. However, usually the radius of the cyclotron motion (81 \AA at 10 T) is much larger than the well width, so that the magnetic field can be treated as a small perturbation. It can be easily shown that this perturbation causes additional confinement for both electron and hole subbands, which results in the *decrease* of the band overlap. Hence an in-plane magnetic field tends to decrease the number density of e - h pairs, leading to a reduction in the intensity of the e - X line in favor of e -CR.

5. FIR laser magnetospectroscopy

FIR laser magnetospectroscopy of sample 6 ($x=0.1$) has exhibited rich spectra. An optically pumped FIR molecular gas laser was used to generate FIR radiation at wavelengths of 61.6 , 70.5 , 96.5 , 118.8 , 250.0 , 393 , and $432 \mu\text{m}$. In Fig. 14 six representative traces are shown for five different FIR laser wavelengths. The top four traces were taken with unpolarized FIR radiation, whereas the bottom two traces were taken with circularly polarized radiation. At least three absorption lines are clearly observed for each wavelength; we have attached arrows to only those features whose resonance fields can be easily determined. In order to determine the origin of the lines unambiguously, positions of the transmission minima are plotted in Fig. 8(a), together with results obtained by Fourier-transform magnetospectroscopy of the same sample at the same temperature. It is clearly seen that some of the features are e -CR and others correspond to the e - X line. The most important point to note is that the lines that are observed as broad low-energy tails in Fourier-transform spectra are observed clearly as (reasonably sharp) minima in the laser spectra. This is because these lines (one

at 3.5 – 4 T and another at 5.5 – 6 T) have extremely large slope vs field. Finally, circular polarization measurements were performed to distinguish between electronlike and holelike transitions unambiguously. In Fig. 14 two transmittance spectra at a wavelength of $250.0 \mu\text{m}$ are displayed for electronlike and holelike circular polarizations, respectively. The data were obtained with a circular polarizer that was 65% efficient. It can be clearly seen that the e - X line and e -CR are electronlike and the h - X line is holelike.

IV. DISCUSSION

A. Anomalies in cyclotron resonance

1. “Antinonparabolic” behavior

In “semimetallic” samples, sample 5 ($x=0.2$) and sample 6 ($x=0.1$), in which the bottom of the InAs conduction band is lower in energy than the top of the $\text{Al}_x\text{Ga}_{1-x}\text{Sb}$ valence band, we have observed several types of anomalous behavior of e -CR. Some of these anomalies may be characterized by the term “antinonparabolic effects” since they are in a certain sense *opposite* to the well-known band nonparabolicity effects. As described below, these effects manifest themselves in the carrier-density (or the Fermi energy E_F) dependence of the low-field cyclotron mass and in the magnetic-field dependence of the high-field cyclotron mass. Consideration of all the bizarre observations leads us to the idea that the electron confinement mechanism in type-II broken-gap QW’s is totally different from that in type-I QW’s and type-II staggered QW’s, and that coexisting holes may play a role in determining (renormalizing) the mass of electrons in type-II broken-gap QW’s through the Coulomb interaction between them.

In the more common type-I semiconductor QW’s in low perpendicular magnetic fields ($\hbar\omega_c \ll E_F$), the cyclotron mass of confined carriers is directly related to the value of $E_1 + E_F$, where E_1 is the energy of the lowest subband due to the confinement in the growth direction, provided the well width is not extremely narrow and the mass enhancement effect due to the wave-function penetration into the barriers can be neglected. A larger mass for a QW with a larger electron sheet density is expected under these conditions because of nonparabolicity. In QW’s made from materials with large conduction-band nonparabolicity like InAs, this effect is very pronounced;^{10,11} CR masses are much larger than the bulk band-edge mass [$0.024m_0$ (Ref. 47)]. However, this simple expectation breaks down for samples 5 and 6 in the present work. In Table II we summarize the low-field cyclotron masses obtained for four different samples, both before and after LED illumination, together with the corresponding densities. As can be seen, there is a systematic difference between samples 5 and 6 and samples 1 and 3. For samples 5 and 6, the low-field mass is *heavier* after illumination, although the electron density is *lower* after illumination; on the other hand, for samples 1 and 3, which are type-II staggered “semiconducting” QW’s, the mass after illumination is *lighter* than that before illumination. The latter behavior can be understood in terms of the usual conduction-band nonparabolicity. It should be also noted that samples 1 and 3 have much lighter masses than samples 5 and 6, although they have similar densities and the same well width.

TABLE II. Low-field cyclotron mass for four samples both before and after LED illumination, together with corresponding electron densities. SC, semiconducting; SM, semimetallic. It can be seen that “semimetallic” samples exhibit *heavier* masses after illumination, inconsistent with nonparabolicity.

Sample no.	x	Illumination condition	SC or SM	Density ($\times 10^{11} \text{ cm}^{-2}$)	Low-fields mass (in units of m_0)
1	1.0	Before	SC	9.5	0.0349 ± 0.0005
		After	SC	6.0	0.0338 ± 0.0005
3	0.5	Before	SC	8.5	0.0341 ± 0.0001
		After	SC	6.1	0.0315 ± 0.0001
5	0.2	Before	SC/SM	6.4	0.0349 ± 0.0003
		After	SM	5.8	0.0368 ± 0.0005
6	0.1	Before	SM	6.2	0.0378 ± 0.0003
		After	SM	5.5	0.0395 ± 0.0005

When the magnetic field value is increased, and the quantum limit is approached, the spectroscopic cyclotron masses (defined by $m^* = eB/\omega_c$, where ω_c is the experimentally obtained resonance frequency) are no longer constant with field. They are generally expected to be a strong function of the Landau-level filling factor, because different transitions have different spectroscopic masses due to the band nonparabolicity: spectroscopic effective masses and effective g factors are energy dependent. In that case, the field dependence of the masses should reflect the movement of E_F with applied magnetic field. This effect has been very clearly observed in earlier work on InAs-AlSb QW's,^{10,11} and also in semiconducting samples in the present work. However, for samples 5 and 6, as shown in Figs. 5(a) and 8(a), respectively, the field-dependence of the high-field spectroscopic cyclotron mass in the presence of the e - X line is very unusual. The mass oscillates strongly with field, as expected, but in an unexpected way: it abruptly shifts to *heavier* values at even integer filling factors; between two such adjacent shifts, the mass clearly *decreases*. In order to compare qualitatively the opposite behaviors for two cases—nonparabolic and antinonparabolic—the characteristic ways in which splittings occur are shown pictorially in Fig. 15. We emphasize that the semiconducting samples exhibit the *usual* nonparabolic effects.

Finally, and most strikingly, the detailed studies with a FIR laser (Sec. III B 5) have unambiguously shown that there exist FIR lines whose transition energies extrapolate to zero at *finite* magnetic fields but quickly approach the classical CR with *extremely large slope vs magnetic field* [see Fig. 8(a)]. None of these anomalous magneto-optical phenomena have been observed in any existing 2D semiconductor systems to the best of our knowledge, and require us to reconsider the electron subband structures in the “semimetallic” regime both in the absence and the presence of magnetic fields.

2. Hybridization of in-plane dispersion relations

Very interesting results of a series of theoretical investigations on InAs/GaSb type-II broken-gap heterostructures have been reported by Altarelli and co-workers,^{15–17} which appear to be consistent with part of the present experimental results for samples 5 and 6. It is particularly interesting that the existence of magneto-optical transitions having energies

that extrapolate to zero at finite magnetic field, but rapidly approach CR with increasing magnetic field, has been predicted;¹⁶ however, to date such lines have not been unambiguously observed experimentally, to our knowledge. The essential idea¹⁵ on which calculations are based is that conduction-band states in InAs and valance-band states in (Al)GaSb are coupled through boundary conditions on the envelope functions (and their derivatives) at the InAs-(Al)GaSb interface. The coupled in-plane dispersion relations, computed in the framework of the envelope-function approximation, were shown to obey a no-crossing rule which

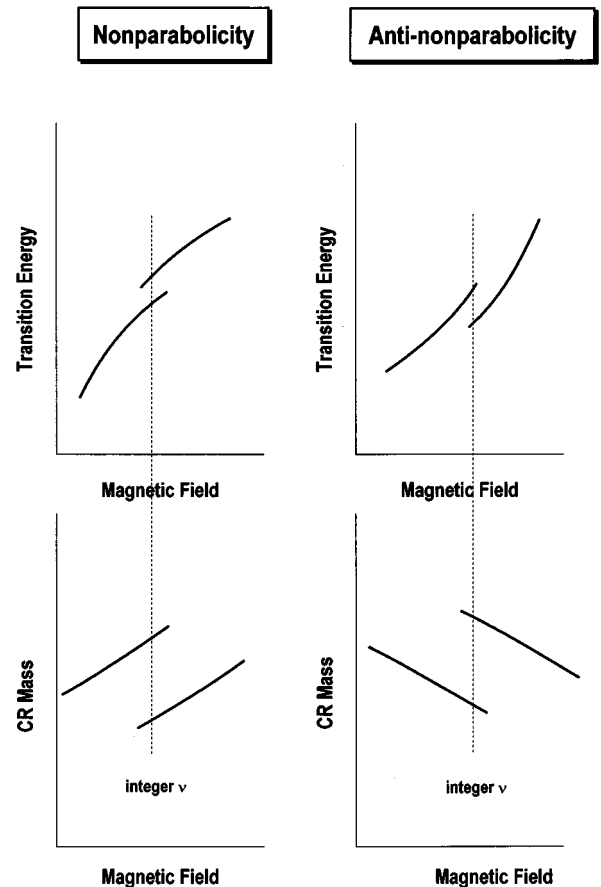


FIG. 15. Characteristic difference in the way in which a splitting occurs between parabolic and antiparabolic cases.

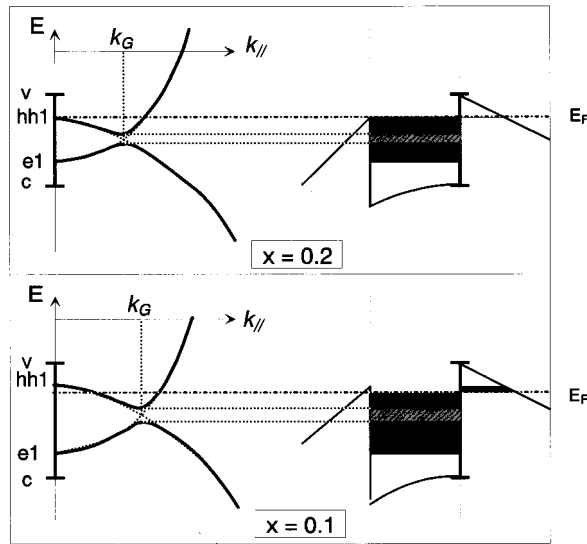


FIG. 16. Schematic energy-band diagram in the k -parallel plane (left panel) and in real space (right panel) for “semimetallic” InAs-Al_{*x*}Ga_{1-*x*}Sb single QW structures ($x=0.2$ and 0.1).

opens up small (≤ 10 meV) energy gaps between conduction-band-like and valence-band-like subbands.¹⁵ These results strongly indicate that in an *intrinsic* sample no truly semimetallic band structure exists; the semimetallic behavior observed for real systems thus arises from extrinsic effects.

We believe that anomalies observed in the present work arise from the fact that the positions of E_F in samples 5 and 6 are close to the above-mentioned energy gaps. This situation has never been achieved experimentally, primarily due to the pinning of E_F far above the gaps in the InAs/GaSb samples studied previously. In Fig. 16 schematic diagrams of band structure for InAs/Al_{*x*}Ga_{1-*x*}Sb ($x=0.2$ and 0.1) both in k space (left panel) and in real space (right panel) are shown. We assume that the mechanism that determines the position of E_F is predominantly the surface-donor-pinning mechanism^{17,18} since the top barriers in all the samples studied are very thin (15 nm). This results in asymmetric QW’s in real space, as shown in the figure; we assume that the holes are confined only at the “bottom” interface (to the right in the figure). In k space, energy vs in-plane wave vector (k_{\parallel}) relations show small band gaps at finite k_{\parallel} , i.e., at $k_{\parallel}=k_G$. For sample 5 ($x=0.2$), before LED illumination, E_F is slightly higher than the band extremum at $k=0$; no holes exist. However, after LED illumination, E_F is lowered toward the gap, leading to the coexistence of electronlike and holelike Fermi surfaces; thus the system is now a “semimetal.” Hence dramatic changes in magneto-optical properties due to illumination can be expected. For sample 6 ($x=0.1$) there is a larger band overlap, which makes it possible for E_F to lie always below the extremum at $k_{\parallel}=0$. It can be understood how illumination in this case results in an increase (decrease) in the hole (electron) density, consistent with experimental observations.

Although we have not investigated samples with $x=0$, we can predict very interesting situations (Fig. 17) based on the idea presented above. It is possible for E_F to lie both above [Fig. 17(a)] and below [Fig. 17(b)] the gap because of the

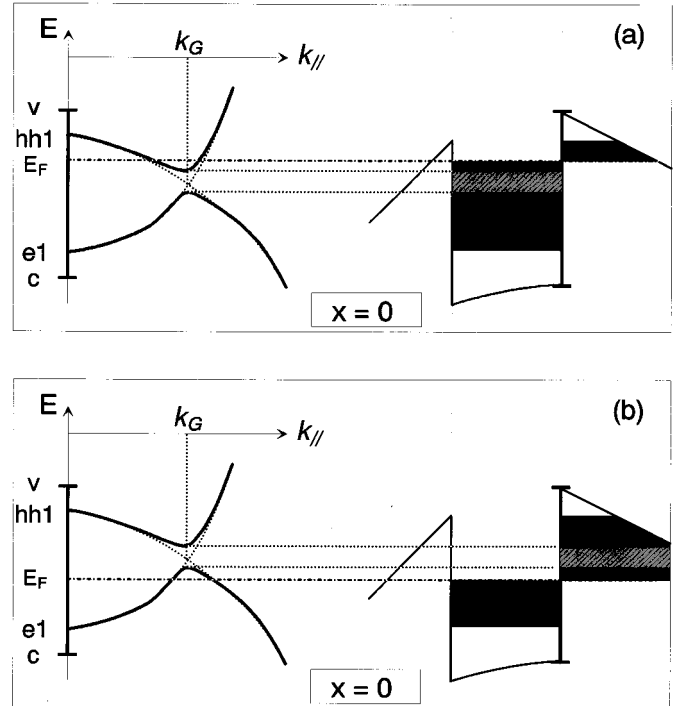


FIG. 17. Schematic energy-band diagram in the k -parallel plane (left) and in real space (right) for an InAs-GaSb single QW structure. (a) The case where the Fermi level lie above the hybridization gap and (b) below the gap.

relatively large band overlap (~ 150 meV) in this case. Both of these situations can be called “semimetallic,” but they should have completely different carriers dominating the conductivity with different natures; e.g., holes in the former case are populated in a pocket near $k_{\parallel}=0$, but in the latter case they are in the donutlike pocket near $k_{\parallel}=k_G$. Experimental distinction between these two situations has not been reported, but we believe that improvements in sample quality in terms of the control of E_F will lead to such observations. In particular, samples whose E_F is very close to the gap should have carriers that have unusual properties, since those carriers should have mixed character of the InAs conduction band and the GaSb valence band. In fact, recent results of FIR magneto-optical studies on InAs/GaSb systems in other laboratories^{48–50} have shown strong CR oscillations,^{48–50} antinonparabolic behavior,⁴⁸ and a line at higher frequency than CR in some situations.^{48,49} Some of these results appear to be similar to the results we have obtained for sample 6 ($x=0.1$), but there are also some significant differences. We believe that the small band overlap in our system coupled with the position of E_F led to the first realization of a situation in which the predicted unusual behavior is directly observed.

The Landau-level spectrum based on the above picture is very complex,¹⁶ reflecting the “antinonparabolic” nature of the E vs k_{\parallel} relationship which results from the band overlap and band repulsion. However, the most essential points can be qualitatively understood by a simple two-band model assuming parabolic conduction-band-like and valence-band-like bands. In Fig. 18(a), Landau levels for interacting electronlike and holelike bands, calculated within such a two-band model, are presented. The intraband transition energy

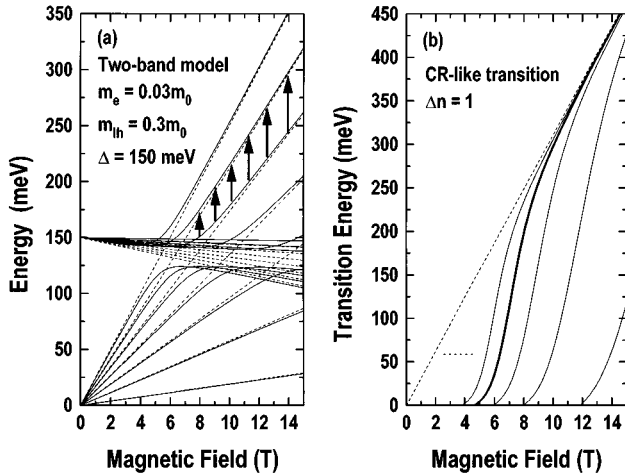


FIG. 18. (a) Schematic Landau-level spectrum calculated for a two-band system. The coupling between the two bands leads to unusual magnetic-field dependence: electronlike levels at low fields become holelike at high fields, and vice versa. (b) Transition energy between adjacent energy levels calculated from (a). The existence of lines whose transition energy goes to zero at finite magnetic fields, consistent with the experimental results [see Fig. 8(a)], is clearly seen.

between two adjacent energy levels, namely the CR-like transition, is shown in Fig. 18(b). The transitions indicated by the arrows in Fig. 18(a) correspond to the transition energies shown by the thick solid line in Fig. 18(b). The calculated results are consistent with our experimental results in two major areas: (1) because the conduction-band bottom is lower in energy than the top of the valence band, the interaction is *opposite* to the usual $\mathbf{k} \cdot \mathbf{p}$ interaction between the bands in narrow-gap semiconductors; this leads to antinonparabolic effects such as a *decrease* in cyclotron mass with increasing magnetic field and an increase in energy separation between adjacent levels with increasing Landau index; and (2) there exist lines that have unusually large slope vs magnetic field and become normal CR at high fields, strongly reminiscent of the experimental observations in the present work [see Fig. 8(a)].

An important question arises as to the pictures in Figs. 16 and 17: what value would be obtained for carrier densities from CR measurements? Since the electrons *below* the gap are *inert*, they cannot participate in electrical conduction, and hence should not be counted. The value of k_F does *not* reflect the number density through the equation $k_F = (2\pi n)^{1/2}$, as expected for usual 2D carriers. Instead, the real electron density, which could be very small if we do not count the inert electrons, should be obtained from the relation, $k_{Fe}^2 - k_{Fh}^2 = 2\pi n$. However, the apparent CR intensity should always be larger than expected from the real electron density because of the large value of k_F , which corresponds to a large Landau index. It is important to note that the oscillator strength of CR increases with the Landau index in such a way that the CR intensity invariably gives the *total* electron density despite the fact that in CR we can probe only electrons across E_F . Therefore, electron densities obtained from CR inevitably contain the inert electrons. This is particularly true when the Fermi level is far away from the hybridization gap, and the energy vs k relation in the vicinity of k_F is very

similar to what it would be without the coupling. When the magnetic field becomes strong, however, more and more Landau levels successively depopulate, and finally the system approaches a point where the effects of the hybridization are significant. Then the simple oscillator strength vs Landau index relation breaks down, and notable changes (decrease) in CR intensity should be expected. The remarkable field-induced reduction in CR intensity observed for sample 5 [Fig. 5(b)] could be explained in this way.

As we saw, the theoretical model proposed by Altarelli and co-workers^{15–17} can successfully explain some part of the present experimental results. However, several important points remain unresolved in this framework: e.g., CR linewidth and amplitude oscillations, the temperature dependence of the CR oscillations, and the appearance of the X lines. It appears that some of the experimental aspects cannot be understood in terms of one-electron theories without invoking many-body effects. These issues will be discussed in the remainder of this paper.

3. CR oscillations—many-body effect or band-structure effect?

The filling-factor-dependent CR linewidth oscillations in quasi-2D systems, observed over the years by *some* workers in *some* systems, has provoked a great deal of controversy. In the past there have been numerous attempts, both theoretical and experimental, to elucidate this and other filling-factor-dependent properties of 2D CR, but a complete understanding is still elusive. The filling-factor-dependent screening of impurity scatterers by 2D electron gases (2DEG's) (Refs. 39–41) and unresolved nonparabolicity-induced CR splittings⁴² have been suggested as possible interpretations to understand some of the experimental data. By comparing the present results with other theoretical and experimental reports,^{10,11,39–42} we shall examine these possibilities for the origin of the oscillations in the present work, as well as explore possible alternative interpretations.

a. Filling-factor-dependent screening of ionized impurities by 2DEG's. The screening properties of a 2DEG in a strong perpendicular magnetic field, and their effects on CR linewidth have been theoretically studied by several authors.⁴¹ In a strong magnetic field the electronic energy levels are completely quantized, and a singular, discrete density of states arises in the ideal cases. Since the strength of the screening is determined by the density of states at the Fermi energy, which depends sensitively on Landau-level broadening in real systems, which in turn is determined by the screening, these effects must be determined self-consistently. The screening is strongest when the highest occupied Landau level is half-filled (odd-integer filling factors), and weakest when it is nearly filled or empty (even-integer filling factors), assuming *negligible* spin splitting. Hence this leads to a variation of Landau-level width with the Landau-level filling factor. This effect has been invoked in many cases to explain anomalies in CR line shape in quasi-2D systems.^{38,51–58}

Experimental observation of CR linewidth oscillations with filling factor was first reported, and interpreted with the above screening idea, by Englert *et al.*⁴⁰ In a 2DEG in GaAs/Al_xGa_{1-x}As heterojunctions, they observed linewidth maxima near $\nu=4$ and 2. They also observed that the line-

width oscillation became weaker with increasing temperature, approaching the mean value between the maxima and the minima at the highest temperature (~ 40 K), similar to the present observations. Heitmann, Ziesmann, and Chang³⁹ observed very pronounced oscillations of CR amplitude and width for electrons in InAs/GaSb single QW's. The oscillations were much larger than the earlier results for GaAs/Al_xGa_{1-x}As.⁴⁰ Maximum linewidths and minimum amplitudes occurred under the condition that the highest Landau level (both spin states) is fully filled, corresponding to *even*-integer filling factors. These authors also attributed the oscillations to filling-factor-dependent screening of the 2DEG. Subsequent studies on GaAs/Al_xGa_{1-x}As systems, however, produced a confusing array of sample-dependent results.^{38,51-58} At present the only experimental results that are fully consistent with the idea of screening are those of Ref. 39 in InAs/GaSb/QW's—a "semimetallic" system.

The present results, however, pose serious problems for this interpretation. First, the observability of the oscillations in the present work is correlated only with the existence of band overlap, *not* with impurities; grown under the same conditions, all the samples should have similar residual impurity densities irrespective of whether they are semiconducting or semimetallic. In addition, samples 1 and 2, which have lower mobilities (more scatterers) than samples 5 and 6, *no* oscillations were observed. Second, as shown by Mendez, Esaki, and Chang,⁵⁹ the important filling factor for a 2D *e-h* system should be the difference $\nu_e - \nu_h$, not the *electron* filling factor ν_e ; the variation of the density of states at the Fermi energy is *not* simply connected to a single parameter ν_e . Thus it can be concluded that the filling-factor-dependent screening of ionized impurities by the 2DEG is *not* the origin of the strong electron CR oscillations observed in the present work.

b. Nonparabolicity and anti-nonparabolicity. An alternative explanation for the CR oscillations was proposed by Hansen and Hansen,⁴² who showed that nonparabolicity in conjunction with occupation effects produces an oscillatory behavior of CR mass, linewidth, and amplitude. They performed calculations for an InAs QW and a GaAs/Al_xGa_{1-x}As heterojunction. Their results resemble to the experimental results of Heitmann, Ziesmann, and Chang³⁹ in some qualitative aspects. However, there is a very important difference: the calculations showed that maximum linewidths and minimum amplitudes occur at *odd* filling factors, whereas these features were observed at *even* filling factors.³⁹ More recently two groups independently performed CR measurements on high-mobility InAs/AlSb single QW's,^{10,11} clearly showing maximum linewidths (or larger splittings) at *odd* filling factors, inconsistent with the screening idea but consistent with the nonparabolicity interpretation.⁴² Scriba *et al.*¹⁰ concluded that the oscillations result from unresolved splittings caused by nonparabolicity, based on the fact that they observed strong oscillations instead of splittings in early samples with low mobilities ($\leq 10^5$ cm²/V s).

It is obvious that this interpretation does not apply to the present results (*or* to those of Ref. 39), since the pronounced

oscillations observed in samples 5 and 6 are *absent* in semiconducting samples. In addition, linewidth maxima occur at *even* filling factors. However, unresolved CR splittings due to *antinonparabolicity* shown in Figs. 8(a), 15, and 18, instead of nonparabolicity, can also produce very similar oscillatory linewidths, since they are also correlated with filling factor. At an even integer filling factor two CR lines are expected (neglecting possible spin splitting): one (high energy) has a normal slope and the other (low energy) has an unusually large slope vs field. With increasing field, the former decreases and the latter increases in intensity rapidly, since the Fermi energy moves from one Landau level to another around this filling factor. As the field increases further, the low-energy line becomes the only feature with a normal slope vs field, until the next even filling factor where it becomes the high energy line, and a low-energy line is expected to appear. Thus if these lines are unresolved, in a similar manner to nonparabolicity-induced oscillations, the CR linewidth oscillates with the filling factor. Experimental results, at least those at 4.2 K, appear to be qualitatively consistent with this model.

However, this interpretation fails to explain the anomalous temperature dependence: the mass shifts with temperature toward an *average* mass, the direction of which critically depends on the filling factor, and the dramatic *line narrowing* with *increasing* temperature with a concomitant decrease in the intensity of the *e-X* line around even filling factors. These effects appear to be outside the realm of single-particle band-structure theories. We thus believe that the observed CR oscillations are in part due to unresolved antinonparabolicity-induced CR splittings, but that some other mechanism, particularly many-body effects, must be invoked to explain all the observed phenomena consistently.

c. Other possible mechanisms. From the above considerations, we are led to explore other possible mechanisms which can give rise to the CR oscillations. As we mentioned, existing single-particle theories appear to fail to explain the anomalous temperature dependence. Particularly, the experimental fact that the cyclotron mass at high temperature approaches a value which is *independent* of magnetic field strongly suggests that the low-temperature masses are affected by correlation effects, which are more and more important at lower temperatures. An important point to note is that Kohn's theorem⁶⁰ is broken by the existence of holes (i.e., the existence of the Coulomb attraction between electrons and holes). In this section we consider two types of *e-h* interactions: scattering and binding; these may play significant roles in determining CR linewidth.

Before considering each case, first let us discuss a general property of 2D *e-h* systems in strong perpendicular magnetic fields—namely, carrier density oscillations with magnetic field. This was theoretically studied by Lerner and Lozovik⁶¹ and Bastard *et al.*⁴⁶ The basic idea is that in order to retain the charge neutrality condition while keeping the chemical potential constant throughout the system, electrons must move back and forth between conduction- and valence-band states, which overlap, with magnetic field; this leads to a variation of both electron and hole densities.

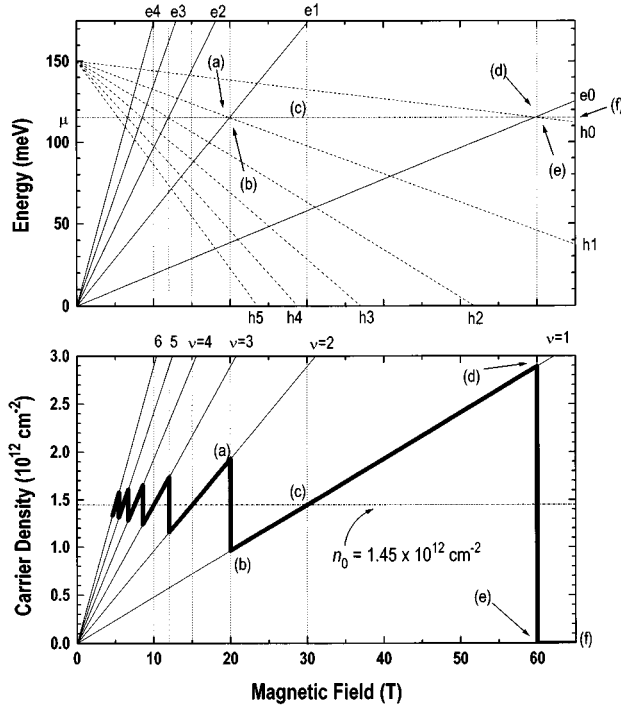


FIG. 19. The Landau-level energy (upper panel) and carrier density (lower panel) as functions of magnetic field for an ideal 2D semimetal (see text). The parameters used are $m_e^* = 0.03m_0$ and $m_h^* = 0.1m_0$, and the zero-field band overlap $\Delta_0 = 150$ meV. A Fermi energy of 115 meV is obtained from these parameters.

Here we consider an ideal system in which there are two parabolic bands, one of which is conduction-band-like and the other valence-band-like, with different masses, m_e^* and m_h^* , with a band overlap $\Delta(B)$ which is a function of magnetic field, and an equal density of electrons and holes, i.e., $n = n_e = n_h$ (or equivalently, $\nu = \nu_e = \nu_h$). The field-dependent overlap $\Delta(B)$ is simply the energy difference between the lowest electronlike Landau level and the highest holelike Landau level, and is determined by the relation $\Delta(B) = \Delta_0 - \hbar\omega_{ce}/2 - \hbar\omega_{ch}/2 = \Delta_0 - \hbar\omega_c/2$, where $\hbar\omega_c = \hbar\omega_{ce} + \hbar\omega_{ch}$, $\omega_{ce} = eB/m_e^*$, $\omega_{ch} = eB/m_h^*$, and $\Delta_0 \equiv \Delta(B=0)$ is the band overlap at zero field. The zero-field carrier density n_0 ($= n_{e0} = n_{h0}$) is determined by the effective masses of electrons and holes through the equation $\Delta_0 = E_{Fe} + E_{Fh} = \hbar^2 \pi n_{e0} / m_e^* + \hbar^2 \pi n_{h0} / m_h^* = \hbar^2 \pi n_0 / \mu$, where $\mu = (m_e^{*-1} + m_h^{*-1})^{-1}$ is the reduced mass. If, for instance, we choose the parameters $m_e^* = 0.03m_0$, $m_h^* = 0.1$, and $\Delta_0 = 150$ meV, then we obtain $n_0 = 1.45 \times 10^{12} \text{ cm}^{-2}$.

At finite magnetic field, the carrier density is determined by counting the number of Landau levels contained in the energy range $\Delta(B)$, when the inequality $(\nu-1)\hbar\omega_c < \Delta(B) < \nu\hbar\omega_c$, where ν is an integer, holds; the carrier density $n(B) [= n_e(B) = n_h(B)]$ is given by $n(B) = \nu \times n_B = \nu \times eB/h \times 2$, where $n_B \equiv eB/h \times 2$ is the degeneracy of each Landau level (the factor 2 takes account of the spin degeneracy of each Landau level). In Fig. 19 carrier density oscillations, calculated by the above equations, are shown in the lower panel for this ideal system, together with a Landau-level spectrum (in the upper panel). In the upper panel the solid (dashed) lines correspond to electron (hole) Landau

levels. It is seen that the carrier density oscillates around the zero-field value $1.45 \times 10^{12} \text{ cm}^{-2}$ with increasing B , exhibiting very large jumps when the number of levels that are completely occupied changes. The amplitude of the oscillation continuously increases with B , until finally the carrier density drops to zero at 60 T, which corresponds to a field-induced semimetal-semiconductor transition. It is interesting to note that in this ideal 2D e - h system the Fermi energy does not oscillate with field while the density does, contrary to the usual 2D electron systems in magnetic fields, in which the Fermi energy oscillates with field while the electron density is constant.

If the Landau-level widths are sufficiently narrow that this oscillatory carrier density is realized in real systems, the frequency of the scattering of electrons by holes should also oscillate with the field, which may lead to CR linewidth oscillations. In real systems, $n_e > n_h$ is always the case due to extrinsic effects. Hence only part of the total electron density oscillates; i.e., $n_e(B) = n_{e1} + n_{e2}(B)$, where n_{e1} is independent of B , and $n_{e2}(B) = n_h(B)$. The larger the e - h pair density, the stronger the oscillations that are expected; this is consistent with experimental observation that the CR oscillations become stronger with increasing e - h pair density. However, we are not satisfied with this model in two respects. First, in the present experiment we did not see any clear oscillations in the CR *integrated* intensity. The linewidth maxima and amplitude minima occur at the same field, so that their product remains approximately constant, indicating that the electron density does not oscillate significantly. Second, and more importantly, the above picture completely neglects the effects of hybridization, which admixes electron and hole Landau levels in the region of coupling, invalidating any arguments based on separate, independent electron and hole levels.

A model based on e - h binding also can explain oscillatory linewidths. As described in Sec. IV B, at present the only possibility for the origin of the e - X line which is consistent with all the experimental observations is an internal transition ($1s \rightarrow 2p_+$ -like) of stable magnetoexcitons. From the experimental results, particularly those on sample 5, it can be said that the existence of holes (or low enough Fermi energy in the hybridized band structure) is indispensable for the oscillations. Electrons localized in the InAs QW and holes localized in the $\text{Al}_x\text{Ga}_{1-x}\text{Sb}$ barrier(s) interact via their mutual Coulomb attraction, forming stable excitons at sufficiently low temperatures and high magnetic fields. Strong magnetic fields should yield a large binding energy for the 2D excitons and, therefore, are expected to enhance the effectiveness of the Coulomb interaction. In the low-field regime $B < 4$ T, the exciton binding energy increases strongly with field, stabilizing the excitonic state. In the high-field regime 4–7 T, where the quantization of the electron energy levels is significant as evidenced by SdH and QHE measurements, the stability of the excitonic state must depend on ν .^{29,61} This idea is strongly supported by the oscillatory intensity exchange between e -CR and the e - X line, the ν -dependent temperature dependence of the e - X line inten-

sity, and the ν -dependent CR- X separation. The overall tendency is that the excitons are more stable at even ν 's than at odd ν 's.

As we discussed above, there are several possibilities for the origin of the CR oscillations observed in “semimetallic” samples in the present work. Although we cannot clearly pinpoint which mechanism, or which combination of them, is dominant at this point, we believe that e - h interactions (along with this unique band structure) play a central role in the origin of the oscillations.

B. Origin of X lines

1. Possibilities that can be ruled out

In previous FIR magneto-optical studies on InAs/GaSb multiheterostructures⁶² and double heterostructures,⁶³ double CR peaks have been observed, and the higher-energy peaks attributed to the CR of electrons in the second electric subband. However, it is clear that such an interpretation is *not* appropriate for the present *much* narrower QW's, the samples which exhibited double peaks in the earlier work^{62,63} have much larger well widths (≥ 1000 Å) than the present samples (150 Å). From the sample dimensions and densities, it can be estimated that the subband separations for a square well, including the energy-dependent mass, is about 110 meV, and E_F for 6×10^{11} cm⁻² with $m^* = 0.035m_0$ is about 40 meV. It is thus impossible to populate the second subband.

Apart from the simple estimate above, this interpretation is also in strong disagreement with several aspects of the present experimental results. First, for narrow QW's in which electrons are confined by the entire well potential, not at the interface, the upper subband will always have a larger mass than the lower subband, and therefore CR from the upper subband would have a *smaller* slope vs magnetic field. The separation between the two lines should thus increase with increasing magnetic field, whereas the e - X line is nearly parallel to e -CR. Second, if the e - X line was the CR of a second subband, it should appear at low fields and disappear at high fields due to depopulation by magnetic field. This behavior, which is *opposite* to our observations, was observed in GaAs/Al _{x} Ga _{$1-x$} As QW's.⁶⁴ Third, the e - X line should increase with temperature if it is the CR of the second subband, whereas experimentally it decreased. Finally, the postulate of the second subband population cannot explain why the e - X line *increases* in intensity after LED illumination, which reduces E_F . If both lines were due to CR, one from the ground subband and one from an upper subband, they *should both* decrease in intensity as E_F is decreased. The data on sample 5 ($x=0.2$) exhibit the e - X line only *after* illumination *and* at high magnetic fields—behavior which is clearly opposite to that expected for a populated second subband. All of the above argue against the possibility of the population of a second subband.

Residual impurities, more specifically residual shallow donors in the InAs wells, can bind electrons and yield an absorption line which lies above e -CR in energy and is nearly parallel to CR in energy vs field in the high-field limit. However, the existence of such a large density of electrons ($> 10^{11}$ cm⁻²) in the wells precludes the formation of neutral

donors (D^0), negative donor ions (D^-) (Ref. 65) being the only possibility; this fact makes this interpretation for the e - X line very unlikely. The binding energy of hydrogenic *neutral* donors in InAs is very small ($Ry^* = 1.67$ meV) because of its small electron effective mass. In addition, the binding energy of D^- is much smaller— $0.055Ry^*$ in the three-dimensional case. The increase of binding energy due to confinement can be estimated from results for a GaAs QW with a width of 100 Å,⁶⁶ where the zero-field binding energy of D^- is about $\frac{1}{3}Ry^*$ for impurities at the well center. At 9 T, which is in the high-field limit, this value becomes approximately $\frac{2}{3}Ry^*$. Using these (very optimistic) values for InAs wells, the binding energy of D^- is estimated to be at most 1.1 meV—still much smaller than the experimentally obtained value of ~ 4 meV.

The very symmetric line shapes for the e - X line also oppose the idea of an impurity transition. Residual donors in this case could be expected to be distributed randomly throughout the InAs wells. However, unless the donors are δ doped in the center of the wells, the impurity absorption lines should always have an asymmetric line shape broadened to lower energies, since off-center impurities have reduced binding energies.⁶⁷

More importantly, the e - X line is observed only *in the samples that are semimetallic* (and in the case of sample 5 only *after* illumination which creates holes); the observability of the e - X line is correlated only with the existence of holes (or the overlap of the bands), *not* the existence of impurities. There was no evidence of the X lines in any of the semiconducting samples ($x=0.4, 0.5, 0.8,$ and 1.0) under any conditions, although the background impurity density is nominally constant for all the samples; also, two of them (samples 1 and 2) have lower mobilities (so possibly more residual impurities) than samples 5 and 6. In addition, the observation of the h - X line only in the strongly semimetallic sample is completely inconsistent with shallow donor impurities associated with InAs.

An absorption line due to the excitation of quasi-2D magnetoplasmons should appear at energies above CR, and have a field dependence nearly equal to CR in high magnetic fields. However, in the Faraday geometry, coupling of FIR light to the plasmon modes at finite wave vector \mathbf{k} requires a well-defined periodic lateral modulation, which does not exist in the present experiment. Sample inhomogeneity could also contribute to the plasmon excitation,⁶⁸ but it is unlikely to result from, say, random impurity potentials. If inhomogeneity is responsible for the excitation, a well-defined peak is impossible, unless the inhomogeneity happens to have a well-defined periodicity, which seems to us to be pathological.

Again, the strongest argument against this interpretation is the fact that the e - X line does not appear in *any* of the semiconducting samples, in particular in sample 3, which has the largest electron density (hence the largest plasmon frequency), as well as the highest mobility. In addition, the fact that the e - X line appears only after LED illumination (lower electron density) for sample 5 also argues against the magnetoplasmon interpretation. Data on semiconducting samples with $x=1.0, 0.8,$ and 0.4 (samples 1, 2, and 4), which have lower mobilities than samples 5 and 6 and consequently

more possible inhomogeneity and scatterers, did not show any sign of the e - X line.

Finally, if we assume that the e - X line is due to magnetoplasmon excitation, its transition frequency $\omega = (\omega_c^2 + \omega_p^2)^{1/2}$, where ω_c and ω_p are the cyclotron and plasma frequencies, respectively. However, using the experimentally obtained values for ω and ω_c at 7 T gives a zero-field transition energy $\omega_p \sim 100 \text{ cm}^{-1}$, whereas experimentally the e - X -line transition energy approaches a very small intercept at zero field (less than 20 cm^{-1}), qualitatively different behavior. Therefore, we can rule out this possibility.

Spin-resolved 2D CR, first reported for InAs/AlSb QW structures,^{10,11} exhibits two (or more) peaks at certain fields, but the energy separation between the two lines should be much smaller than the CR- X separation (see also Fig. 3). It is possible that the conduction band splits into two branches even at zero magnetic field, due to strong built-in electric field in the growth direction, resulting from the asymmetry of the QW structure, combined with the strong spin-orbit coupling.⁶ However, all the samples possess this possibility equally—again, inconsistent with the appearance of the X lines only in the semimetallic samples. Moreover, if spin were really the cause of the two peaks, the separation between them should increase with field, especially at high magnetic fields. Furthermore, in spin-resolved CR a low-energy line should disappear and be replaced by a high-energy line at integer (even or odd) ν 's, clearly different from the behavior of the e - X line.

Warburton *et al.*⁵⁰ recently reported an observation of two electron CR lines in p^+ asymmetric InAs/GaSb/AlSb single-quantum-well structures (doped in the AlSb). These lines are only observed in the presence of a large density of holes (remote from the electrons in the InAs QW); only a single line is observed in a similar structure doped n^+ in the AlSb near the InAs QW. The two lines bear some resemblance to CR and the e - X line of the present work. In particular, they exhibit oscillations in amplitude, linewidth, and mass with ν ; the amplitudes of both lines are at a minimum, and the linewidths are at a maximum near even-integer ν 's. These authors argued that the two lines are associated with nonparabolicity-induced splitting between CR transitions originating from two different spin states of the same Landau level (a Δg transition occurring at even-integer ν 's) or two different Landau levels having the same spin (a Δm transition occurring at odd-integer ν 's) with the spin-splitting greatly enhanced and field dependent through the spin-orbit effect and the asymmetry of the structure.⁶⁹ In this picture the ν -dependent oscillations are due to resolving the Δm transitions around odd-integer ν 's, while the Δg transitions around even-integer ν 's are not resolved due to hybridization of the two transitions by e - e interactions between the two sets of electrons.^{70,71,10}

In spite of some superficial similarities, there are several significant differences between these results and the present work. First, unlike the CR line of the present work, neither of the lines extrapolates to zero energy at zero magnetic field. Second, the temperature dependence of the intensities is very different; *both* lines broaden and exhibit a reduction in amplitude, but the integrated intensities are independent of temperature (in the present work, the CR line *narrows* as temperature is increased, and gains integrated intensity at the

expense of the X line). Third, the density of holes is much greater than the density of electrons; the opposite is true in the present work. Fourth, the masses vs filling factor exhibit opposite behavior to that of the present work; between even-integer ν 's the masses *decrease*, and the masses jump *up* at integer ν 's. We offer no alternative explanation for these results, but point out that even if the explanation of Warburton *et al.*⁵⁰ were correct for their data, since the behavior of CR and the X line is significantly different in the important aspects listed above, such an interpretation is inappropriate. In addition, it is difficult to reconcile this interpretation with the fact that semiconducting samples with identical structure and with essentially the same electron density show no signs of the X line or the oscillations.

Interband transitions across the InAs-GaSb interface, namely, transitions from the valence-band states in GaSb to conduction-band states in InAs, have been reported previously in Refs. 62, 72, and 73 for InAs/GaSb multiheterostructures. According to the "simple" picture (as depicted in Fig. 1), such transitions are impossible at zero magnetic field due to the fact that the valence-band states lie higher in energy than the conduction-band states; such transitions should appear only at finite magnetic fields, have a much larger slope vs field than CR, and extrapolate to negative energies at zero field because of the band overlap—qualitatively consistent with the results of Guldner *et al.*⁶² but completely different from the behavior of the X lines. However, in order to consider interband transitions more correctly, the peculiar hybridization of the bands at finite k_{\parallel} must be taken into account explicitly, since the above simple picture totally neglects the small *positive* energy gaps which already exist in such "semimetallic" samples even at zero field. The two-band model of Fig. 18 can be used to calculate transition energies for interband magneto-optical transitions, i.e., $\Delta n = 0$. As can be easily seen from Fig. 18(a), however, the calculated transition energies vs field show an initial rapid *decrease*, followed by a rapid *increase* with a much larger slope than CR; this is clearly *not* the behavior of the e - X line.

2. Intraexcitonic resonance and an excitonic ground state

As shown in Figs. 10 and 12 (temperature dependence), X lines appear to be associated with a bound state, since they increase in intensity with decreasing temperature with concomitant reduction of the CR intensity, which is proportional to the density of free carriers. This bound state can exist only when both electrons and holes, spatially separated, are present, and the strength of the transitions increases with increasing hole density (or decreasing E_F). These experimental facts strongly suggest that electrons and holes are bound in the form of a *stable* excitonic state. Unlike typical excitons, this state is a ground state rather than an excited state of the system, so that it can exist without optical excitation. In fact, many of the experimental observations are qualitatively explainable through the assignment of the e - X and h - X lines to excitonic resonance [$1s \rightarrow 2p_+$ in the low-field notation, and $(00) \rightarrow (11)$ in the high-field notation; the latter is more appropriate in the present case] for electrons and holes, respectively: (1) The excitonic interaction between electrons and holes is strengthened by magnetic fields applied perpendicularly to the plane; thus the intensity of the

e - X line rapidly increases with field (and CR decreases due to removal of free carriers); (2) for semiconducting samples ($x=0.4, 0.5, 0.8,$ and 1.0) neither of the X lines is observed, since there are no holes; (3) for sample 5 the e - X line is observed only after LED illumination, which creates holes (and lowers the Fermi energy into the region of peculiar band structure); (4) for sample 6, both the e - X and h - X lines are stronger and can be observed, and they increase in intensity after illumination, which increases e - h pair density.

The binding energy of the exciton can be estimated to be >4 meV from the CR- X separation in the hydrogenic model. This value is reasonable since spatial separation does not reduce the binding energy significantly due to the long-range nature of the Coulomb interaction, and is consistent with the calculated binding energy for similar spatially-separated e - h systems.^{29,33} The magnetic field should also increase the binding energy substantially,^{29,34} and more detailed calculations including these effects are needed to compare with our data. The slope of the e - X and h - X lines can be understood from simple considerations. For excitons the use of the reduced mass is correct in the low-field limit; however, in the high-field limit appropriate to the present situation ($\gamma=\hbar\omega_c/2Ry^*=1$ corresponds to 1.4 T, where Ry^* is the electron effective Rydberg), it can be shown that the excitonic resonance near electron (hole) cyclotron resonance is determined by the electron (in-plane hole) effective mass, consistent with experimentally obtained energy vs field.

Based on all the above experimental facts and considerations, we conclude that, if their assignment is correct, the observation of the X lines provides the first spectroscopic evidence for the existence of a stable excitonic ground state for a spatially separated e - h system. The existence of excess electrons ($n_e > n_h$) may complicate the problem, but does not alter the conclusion that the X lines originate from the e - h Coulomb interaction. Simple considerations of screening effects may lead to the idea that the excitonic binding energy should be significantly reduced, or the Coulomb interaction should be totally "screened out" due to excess electrons. However, it is important to note that the present situation is very different from, say, modulation-doped GaAs/ $Al_xGa_{1-x}As$ heterostructures, in which there is a large density of electrons, and excitons are usually absent in photoluminescence (PL) spectra. In those systems the density of photocreated holes (10^5 – 10^9 cm⁻², depending on excitation intensity) is many orders of magnitude smaller than that of the electron gas, whereas in the present system the hole density is at least ~ 0.1 of the electron density. In addition, in the presence of high magnetic fields, which quantize the electronic states and thereby make screening ineffective, even in the above-mentioned GaAs/ $Al_xGa_{1-x}As$ systems, excitons appear in the PL. Furthermore, recent results on "screening" of shallow impurities in QW's (Refs. 65 and 74) show that excess electrons can cause a "blue" (rather than "red") shift in the transition energy of the D^- singlet states, contrary to the simple static screening ideas.

Finally, it should be also made clear that the e - X line is a transition arising from neutral excitons (X^0) that are composed of one electron and one hole, not negative excitons (X^-), in which two electrons are bound to one hole, and hence the binding of the second electron is very weak compared to the first one. As we mentioned earlier (Sec. IV B 1),

the binding energy of a second electron in a D^- ion at the center of the well (which has the largest possible binding energy) can be estimated to be at most 1.1 meV. The binding energy of an X^- should be even smaller than this value since holes are mobile; if we assume that the electron mass is $0.04m_0$ and the hole mass is $0.1m_0$, and that the holes are located at the center of the same layer as the electrons, the largest possible binding energy for an X^- is $1.1 \text{ meV} \times 0.1/(0.1+0.04)=0.79 \text{ meV}$. This small value leads to the conclusion that the binding of a second electron by a hole is extremely unlikely in the present experimental temperature range 1.5–50 K.

V. SUMMARY AND CONCLUSIONS

We have carried out FIR Fourier transform and laser magnetospectroscopy in magnetic fields up to 15 T in the energy range between 10 and 450 cm⁻¹ on a set of InAs/ $Al_xGa_{1-x}Sb$ single QW samples in a wide range of Al composition x , $0.1 \leq x \leq 1.0$, covering both "semiconducting" and "semimetallic" regimes. Samples with $x > 0.3$ are "semiconducting," containing only electrons in the InAs QW; samples with $x < 0.3$ are "semimetallic:" electrons and holes coexist with the holes in the $Al_xGa_{1-x}Sb$ at the interface. Distinctly different behavior has been observed in these two regimes. The "semimetallic" case exhibited particularly interesting anomalous magneto-optical properties, indicating the participation of and the interaction between both types of carriers.

Semiconducting samples exhibited sharp CR with splittings due to large conduction-band nonparabolicity, consistent with results of other groups.^{10,11} A negative persistent photoeffect was observed in all samples, and was used to control the Fermi level of the samples over a small range. It was found that the sample with $x=0.2$ is still "semiconducting" before LED illumination but becomes "semimetallic" after illumination due to the decrease of the Fermi level.

We observed very strong filling-factor-dependent oscillations in electron CR linewidth, amplitude, and mass in the "semimetallic" regime. The present results have made clear the fact that the oscillations are correlated with the existence of holes (or the overlap between the InAs conduction band and the $Al_xGa_{1-x}Sb$ valence band), not impurities. Thus the frequently suggested mechanism, the filling-factor-dependent screening of ionized impurities by 2DEG's, is not the origin of the oscillations. This finding resolves some of the discrepancies reported on CR in InAs type-II QW's. We believe that the Coulomb interaction between spatially separated electrons and holes, at least partly, plays a role in the origin of the oscillations.

We have shown that some of the anomalous phenomena observed only in the "semimetal" situation arise from hybridization of in-plane dispersion relations between InAs-like conduction band and $Al_xGa_{1-x}Sb$ -like valence band. Most dramatically, we have seen the appearance of lines whose transition energies extrapolate to zero at finite magnetic field but rapidly approach typical CR with an extremely large slope vs field. We believe that the observation of this behavior in CR is the first conclusive evidence of the resonant coupling between conduction-band states in InAs and valence-band states in (Al)GaSb, in qualitative agreement

with the theories of Altarelli and co-workers.^{15–17} It should be noted that this coupling always opens up an energy gap, making intrinsic (or ideal) “semimetallic” systems semiconducting.

New far-infrared absorption lines (the “X lines”), which have been observed *only* in the “semimetallic” situation at low enough temperatures and at high enough magnetic fields, were ascribed to excitonic resonances [$1s \rightarrow 2p_+$ in the low-field notation, and (00)→(11) in the high-field notation; the latter is more appropriate in the present case]. If this assignment is correct, this work represents the first spectroscopic evidence of the existence of a stable excitonic ground state, in which excitons can exist with no optical pumping.

We anticipate that the experimental findings presented in this paper will stimulate interest in the problem of spatially-separated 2D electron-hole systems in high magnetic fields, and more theoretical calculations, with many-body interactions, will be performed to obtain accurate transition energies of both CR and X lines for this system to compare with our

data. Furthermore, this work should encourage theorists who have predicted various interesting states/phenomena for 2D $e-h$ systems in high magnetic fields.

ACKNOWLEDGMENTS

This work was supported in part by the Office of Naval Research under Grant Nos. N00014-89-J-1673 and N00014-91-J-1939. We would like to thank M. O. Manasreh and R. K. Evans for sample preparation, W. J. Li, G. S. Herold, S. R. Ryu, Z. Jiang, and S. K. Singh for experimental assistance, R. J. Wagner, J. R. Meyer, and B. V. Shanabrook for stimulating discussions on hybridized in-plane dispersion relations and for providing us with unpublished results, Professor B. A. Weinstein, Professor A. Petrou, and Professor J. J. Quinn for useful discussions. One of us (J.K.) acknowledges financial support from the Ishizaka Foundation, Japan. I.L. was supported in part by the National Science Council of Taiwan, the Republic of China.

*Present address: Quantum Institute, Center for Free-Electron Laser Studies, University of California, Santa Barbara, CA 93106-5100. Electronic address: kono@qi.ucsb.edu

†Electronic address: mcombe@acsu.buffalo.edu

‡Present address: Xerox Corporation, 4 Cambridge Center, Cambridge, MA 02142.

Electronic address: cheng@XAIT.Xerox.COM

§Present address: Department of Physics, National Sun Yat-Sen University, Kaohsiung 80424, Taiwan, the Republic of China. Electronic address: ikailo@venus.phys.nsysu.edu.tw

¹G. A. Sai-Halasz, R. Tsu, and L. Esaki, *Appl. Phys. Lett.* **30**, 651 (1977); G. A. Sai-Halasz, L. Esaki, and W. A. Harrison, *Phys. Rev. B* **18**, 2812 (1978).

²For a review, see, e.g., L. L. Chang and L. Esaki, *Surf. Sci.* **98**, 70 (1980); L. L. Chang, *J. Phys. Soc. Jpn.* **49**, Suppl. A, 997 (1979); L. Esaki, *IEEE Quantum Electron.* **QE-22**, 1611 (1986).

³H. Munekata, L. Esaki, and L. L. Chang, *J. Vac. Sci. Technol. B* **5**, 809 (1987); H. Munekata, T. P. Smith III, and L. L. Chang, *J. Cryst. Growth* **95**, 235 (1989).

⁴G. Tuttle, H. Kroemer, and J. H. English, *J. Appl. Phys.* **65**, 5239 (1989); P. F. Hopkins, A. J. Rimberg, R. M. Westervelt, G. Tuttle, and H. Kroemer, *Appl. Phys. Lett.* **58**, 1428 (1991).

⁵I. Lo, W. C. Mitchel, M. O. Manasreh, C. E. Stutz, and K. R. Evans, *Appl. Phys. Lett.* **60**, 751 (1992).

⁶J. Luo, H. Munekata, F. F. Fang, and P. J. Stiles, *Phys. Rev. B* **38**, 10 142 (1988); **41**, 7685 (1990).

⁷T. P. Smith III, H. Munekata, L. L. Chang, F. F. Fang, and L. Esaki, *Surf. Sci.* **196**, 687 (1988).

⁸I. Lo, W. C. Mitchel, and J.-P. Cheng, *Phys. Rev. B* **48**, 9118 (1993); **50**, 5316 (1994).

⁹D. J. Barnes, R. J. Nicholas, R. J. Warburton, N. J. Mason, P. J. Walker, and N. Miura, *Phys. Rev. B* **49**, 10 474 (1994).

¹⁰J. Scriba, A. Wixforth, J. P. Kotthaus, C. R. Bolognesi, C. Nguyen, G. Tuttle, J. H. English, and H. Kroemer, *Semicond. Sci. Technol.* **8**, S133 (1993); J. Scriba, A. Wixforth, J. P. Kotthaus, C. Bolognesi, C. Nguyen, and H. Kroemer, *Solid State Commun.* **86**, 633 (1993).

¹¹M. J. Yang, P. J. Lin-Chung, B. V. Shanabrook, J. R. Waterman, R. J. Wagner, and W. J. Moore, *Phys. Rev. B* **47**, 1691 (1993); M. J. Yang, R. J. Wagner, B. V. Shanabrook, J. R. Waterman,

and W. J. Moore, *ibid.* **47**, 6807 (1993).

¹²J. Kono, B. D. McCombe, J.-P. Cheng, I. Lo, W. C. Mitchel, and C. E. Stutz, *Phys. Rev. B* **50**, 12 242 (1994).

¹³J.-P. Cheng, J. Kono, B. D. McCombe, I. Lo, W. C. Mitchel, and C. E. Stutz, *Phys. Rev. Lett.* **74**, 450 (1995).

¹⁴C. Gauer, A. Wixforth, J. P. Kotthaus, M. Kubisa, W. Zawadzki, B. Brar, and H. Kroemer, *Phys. Rev. Lett.* **74**, 2772 (1995).

¹⁵M. Altarelli, *Phys. Rev. B* **28**, 842 (1983).

¹⁶A. Fasolino and M. Altarelli, *Surf. Sci.* **142**, 322 (1984).

¹⁷M. Altarelli, J. C. Maan, L. L. Chang, and L. Esaki, *Phys. Rev. B* **35**, 9867 (1987).

¹⁸C. Nguyen, B. Brar, H. Kroemer, and J. H. English, *Appl. Phys. Lett.* **60**, 1854 (1992).

¹⁹H. Kroemer, C. Nguyen, and B. Brar, *J. Vac. Sci. Technol. B* **10**, 1769 (1992).

²⁰S. Ideshita, A. Furukawa, Y. Mochizuki, and M. Mizuta, *Appl. Phys. Lett.* **60**, 2549 (1992).

²¹D. J. Chadi, *Phys. Rev. B* **47**, 13 478 (1993).

²²See, e.g., E. W. Fenton, *Phys. Rev.* **170**, 816 (1968); A. A. Abrikosov, *J. Low Temp. Phys.* **10**, 3 (1973); A. A. Abrikosov, *Zh. Eksp. Teor. Fiz.* **65**, 1508 (1973) [*Sov. Phys. JETP* **38**, 750 (1974)]; G. E. W. Bauer, *Phys. Rev. Lett.* **64**, 60 (1990).

²³See, e.g., S. Nakajima and D. Yoshioka, *J. Phys. Soc. Jpn.* **40**, 328 (1976); L. V. Keldysh and T. A. Onishchenko, *Pis'ma Zh. Eksp. Teor. Fiz.* **24**, 70 (1976) [*JETP Lett.* **24**, 59 (1976)].

²⁴I. V. Lerner and Yu. E. Lozovik, *Solid State Commun.* **23**, 453 (1977); *J. Phys. C* **12**, L501 (1979); *Zh. Eksp. Teor. Fiz.* **80**, 1488 (1981) [*Sov. Phys. JETP* **53**, 763 (1981)].

²⁵D. Paquet, T. M. Rice, and K. Ueda, *Phys. Rev. B* **32**, 5208 (1985).

²⁶See, e.g., H. Hasegawa, M. Robnik, and G. Wunner, *Prog. Theor. Phys. Suppl.* **98**, 198 (1989).

²⁷Yu. E. Lozovik and V. I. Yudson, *Pis'ma Zh. Eksp. Teor. Fiz.* **22**, 556 (1975) [*JETP Lett.* **22**, 274 (1975)]; *Solid State Commun.* **19**, 391 (1976); Yu. E. Lozovik and V. N. Nishanov, *Fiz. Tverd. Tela (Leningrad)* **18**, 3267 (1976) [*Sov. Phys. Solid State* **18**, 1905 (1976)].

²⁸D. Yoshioka and H. Fukuyama, *J. Phys. Soc. Jpn.* **45**, 137 (1978).

²⁹Y. Kuramoto and C. Horie, *Solid State Commun.* **25**, 713 (1978).

- ³⁰D. Yoshioka and A. H. MacDonald, *J. Phys. Soc. Jpn.* **59**, 4211 (1990).
- ³¹X. M. Chen and J. J. Quinn, *Phys. Rev. Lett.* **67**, 895 (1991).
- ³²S. Datta, M. R. Melloch, and R. L. Gunshor, *Phys. Rev. B* **32**, 2607 (1985).
- ³³X. Zhu, J. J. Quinn, and G. Gumbs, *Solid State Commun.* **75**, 595 (1990).
- ³⁴X. Xia, X. M. Chen, and J. J. Quinn, *Phys. Rev. B* **46**, 7212 (1992).
- ³⁵T. Fukuzawa, E. E. Mendez, and J. M. Hong, *Phys. Rev. Lett.* **64**, 3066 (1990); J. A. Kash, M. Zachau, E. E. Mendez, J. M. Hong, and T. Fukuzawa, *ibid.* **66**, 2247 (1991).
- ³⁶L. V. Butov, A. Zrenner, G. Abstreiter, G. Böhm, and G. Weimann, *Phys. Rev. Lett.* **73**, 304.
- ³⁷U. Sivan, P. M. Solomon, and H. Shtrikman, *Phys. Rev. B* **68**, 1196 (1992).
- ³⁸For a recent review, see, e.g., A. Petrou and B. D. McCombe, in *Landau Level Spectroscopy*, edited by G. Landwehr and E. I. Rashba, *Modern Problems in Condensed Matter Sciences Vol. 27.2* (North-Holland, Amsterdam, 1991), pp. 679–775; B. D. McCombe and A. Petrou, in *Optical Properties of Semiconductors*, edited by M. Balkanski, *Handbook on Semiconductors Vol. 2* (North-Holland, Amsterdam, 1994), pp. 285–384.
- ³⁹D. Heitmann, M. Ziesmann, and L. L. Chang, *Phys. Rev. B* **34**, 7463 (1986).
- ⁴⁰Th. Englert, J. C. Maan, Ch. Uihlein, D. C. Tsui, and A. C. Gossard, *Solid State Commun.* **46**, 545 (1983).
- ⁴¹See, e.g., T. Ando, *J. Phys. Soc. Jpn.* **43**, 1616 (1977); S. Das Sarma, *Phys. Rev. B* **23**, 4592 (1981); R. Lassnig and E. Gornik, *Solid State Commun.* **47**, 959 (1983); T. Ando and Y. Murayama, *J. Phys. Soc. Jpn.* **54**, 1519 (1985).
- ⁴²E. B. Hansen and O. P. Hansen, *Solid State Commun.* **66**, 1181 (1988).
- ⁴³M. Ziesmann, D. Heitmann, and L. L. Chang, *Phys. Rev. B* **35**, 4541 (1987).
- ⁴⁴S. Das Sarma and B. A. Mason, *Phys. Rev. B* **31**, 5536 (1985); X. Wu, F. M. Peeters, and J. T. Devreese, *ibid.* **34**, 2621 (1986).
- ⁴⁵D. M. Larsen, *Phys. Rev. B* **30**, 4595 (1984).
- ⁴⁶For a self-consistent calculation in this simple picture, see, e.g., G. Bastard, E. E. Mendez, L. L. Chang, and L. Esaki, *J. Vac. Sci. Technol.* **21**, 531 (1982).
- ⁴⁷See, e.g., C. R. Pidgeon, D. L. Mitchell, and R. N. Brown, *Phys. Rev.* **154**, 737 (1967).
- ⁴⁸R. J. Wagner *et al.*, *Bull. Am. Phys. Soc.* **40**, 111 (1995); and (private communication).
- ⁴⁹R. A. Stradling (private communication).
- ⁵⁰R. J. Warburton, B. Brar, C. Gauer, A. Wixforth, J. P. Kotthaus, and H. Kroemer, *Solid State Electron.* **40**, 679 (1996).
- ⁵¹Z. Schlesinger, S. J. Allen, J. C. M. Hwang, P. M. Platzman, and N. Tzoar, *Phys. Rev. B* **30**, 435 (1984).
- ⁵²Z. Schlesinger, W. I. Wang, and A. H. MacDonald, *Phys. Rev. Lett.* **58**, 73 (1987).
- ⁵³K. Ensslin, D. Heitmann, H. Sigg, and K. Ploog, *Phys. Rev. B* **36**, 8177 (1987).
- ⁵⁴W. Seidenbusch, E. Gornik, and G. Weimann, *Phys. Rev. B* **36**, 9155 (1987).
- ⁵⁵E. Batke, H. L. Störmer, A. C. Gossard, and J. H. English, *Phys. Rev. B* **37**, 3093 (1988).
- ⁵⁶J. Richter, H. Sigg, K. v. Klitzing, and K. Ploog, *Phys. Rev. B* **39**, 6268 (1989).
- ⁵⁷R. J. Nicholas, M. A. Hopkins, D. J. Barnes, M. A. Brummell, H. Sigg, D. Heitmann, K. Ensslin, J. J. Harris, C. T. Foxon, and G. Weimann, *Phys. Rev. B* **39**, 10 955 (1989).
- ⁵⁸J.-P. Cheng and B. D. McCombe, *Phys. Rev. B* **44**, 3070 (1991).
- ⁵⁹E. E. Mendez, L. Esaki, and L. L. Chang, *Phys. Rev. Lett.* **55**, 2216 (1985).
- ⁶⁰W. Kohn, *Phys. Rev.* **123**, 1242 (1961).
- ⁶¹I. V. Lerner and Yu. E. Lozovik, *J. Phys. C* **12**, L501 (1979).
- ⁶²Y. Guldner, J. P. Vieren, P. Voisin, M. Voos, L. L. Chang, and L. Esaki, *Phys. Rev. Lett.* **45**, 1719 (1980); Y. Guldner, J. P. Vieren, P. Voisin, M. Voos, J. C. Maan, L. L. Chang, and L. Esaki, *Solid State Commun.* **41**, 755 (1982).
- ⁶³G. M. Sundaram, R. J. Warburton, R. J. Nicholas, G. M. Summers, N. J. Mason, and P. J. Walker, *Semicond. Sci. Technol.* **7**, 985 (1992).
- ⁶⁴See, e.g., K. Ensslin, D. Heitmann, and K. Ploog, *Phys. Rev. B* **37**, 10 150 (1988).
- ⁶⁵J.-P. Cheng, Y. J. Wang, B. D. McCombe, and W. Schaff, *Phys. Rev. Lett.* **70**, 489 (1993).
- ⁶⁶T. Pang and S. G. Louie, *Phys. Rev. Lett.* **65**, 1653 (1991).
- ⁶⁷N. C. Jarosik, B. D. McCombe, B. V. Shanabrook, J. Comas, J. Ralston, and G. Wicks, *Phys. Rev. Lett.* **54**, 1283 (1985).
- ⁶⁸C. Kallin and B. I. Halperin, *Phys. Rev. B* **30**, 5655 (1984).
- ⁶⁹E. I. Rashba, *Fiz. Tverd. Tela (Leningrad)* **2**, 1224 (1960) [*Sov. Phys. Solid State* **2**, 1109 (1960)].
- ⁷⁰N. R. Cooper and J. T. Chalker, *Phys. Rev. Lett.* **72**, 2057 (1994).
- ⁷¹C. M. Hu, E. Batke, K. Köhler, and P. Ganser, *Phys. Rev. Lett.* **75**, 918 (1995).
- ⁷²J. C. Maan, in *Infrared and Millimeter Waves*, edited K. J. Button (Academic, New York, 1983), Vol. 8, p. 163.
- ⁷³L. M. Claessen, J. C. Maan, M. Altarelli, P. Wyder, L. L. Chang, and L. Esaki, *Phys. Rev. Lett.* **57**, 2556 (1986).
- ⁷⁴P. Hawrylak, *Phys. Rev. Lett.* **72**, 2943 (1994).